Supporting Information

The Cleavage of Hg-C bonds of Organomercurials Induced by $Im^{OH}Se$ via Two Distinct Pathways

Mainak Banerjee and Gouriprasanna Roy*

Department of Chemistry, School of Natural Sciences, Shiv Nadar University, NH91, Dadri, Gautam Buddha Nagar, UP 201314, India

Contents:

I. General Experimental

Imidazole, 2-Chloroethyl methyl ether, 4-(Hydroxymercuri)benzoic acid sodium salt (Ar1HgOH, Ar1 = *p*-$C_6H_4CO_2Na$; CAS No.: 138-85-2), MeHgCl, selenium powder were obtained from Sigma-Aldrich chemical company. EtHgCl were obtained from Alfa Aesar. Ethylene chlorohydrine, sodium hydride, and other chemicals were obtained from local companies. All experiments were carried out under anhydrous and anaerobic conditions using standard Schlenk techniques for the synthesis. Ultra-performance liquid chromatography (UPLC) was carried out using an Agilent 6540 accurate–mass Q-TOF LC/MS (Agilent Technologies, U.S.A.). Liquid chromatographic separation was performed at room temperature of 18 °C, using a UPLC C_{18} analytical column (ZORBAX C_{18} Column, 2.1 x 50 mm, 1.8-micron). MS analyses were performed under the following operation parameters: dry gas temperature 350 °C, dry gas (N_2) flow rate 10 L/min, nebulizer pressure 30 psi, V_{cap} 4000 and fragmentor voltage 120 V. Mass spectra were acquired in the positive ion mode by scanning from 110 to 1700 in the mass to charge ratio (m/z). The mobile phase composition used for UHPLC–QTOF MS comprised of a mixture of H_2O (A) and CH_3CN (B), both containing 0.1% HCO_2H, with an optimized linear gradient elution as follows: 0–2 min, 1–5% B; 2–7 min, 5–15% B. The injection volume was 1 μL. The flow rate was set at 0.3 mL/min. The LC/MS/MS experiments were performed with an ESI interface with UHPLC–QTOF MS instrument used for LC/MS analysis. Accurate mass analysis calibration was carried out by ESI-low concentration tuning mix solution provided by Agilent technologies, U.S.A. The accuracy error threshold was set at 10 ppm. All other parameters were similar to LC/MS experimental settings. High performance liquid chromatography (HPLC) experiments were carried out on Agilent 1290 infinity series of LC system (Agilent Technologies, U.S.A.) with photodiode-array/ELSD detector to monitor the degradation of 1:1 mercury conjugated compounds. High performance liquid chromatography (HPLC) experiments were carried out on a Waters Alliance System (Milford, MA) consisting of e2695 separation module and a 2998 photodiode-array detector. The HPLC system was controlled with EMPOWER software (Waters Corporation, Milford, MA). Liquid state NMR spectra were recorded in $CDCl_3$, d_4-MeOH, D_2O, d_6-DMSO as a solvent. ^1H (400 MHz), ^{13}C (100 MHz) , ^{77}Se (76.3 MHz) and ^{199}Hg (71.6 MHz) NMR spectra were obtained on a Bruker Advance 400 NMR Spectrometer using the solvent as an internal standard for ^1H and ^{13}C. Chemical shifts (^1H, ^{13}C) are cited with respect to tetramethylsilane (TMS) and ^{199}Hg NMR spectra are reported in ppm relative to neat Me_2Hg (δ = 0 ppm) and $HgCl_2$ (δ = -1501 ppm for 1 M solution in DMSO-*d6*) was used as external standard Thin-layer chromatography analyses were carried out on pre-coated silica gel plates (Merck) and spots were visualized by UV irradiation. Column chromatography was performed on glass columns loaded with silica gel. Single crystal X-ray diffraction was performed using a Bruker D8 Venture diffractometer operating with Mo Kα radiation and equipped with a CMOS Photon100 area detector.

CAUTION! *Organomercurials are highly toxic to humans, and thus appropriate safety precautions must be taken in handling these toxic organomercurials.*

II. Synthetic Procedures:

Compounds $Im^{Y}Se$ (R = OH, OMe and Me) were synthesized via carbene route from the N, N'-disubstituted imidazolium salts obtained from 1-methylimidazole.

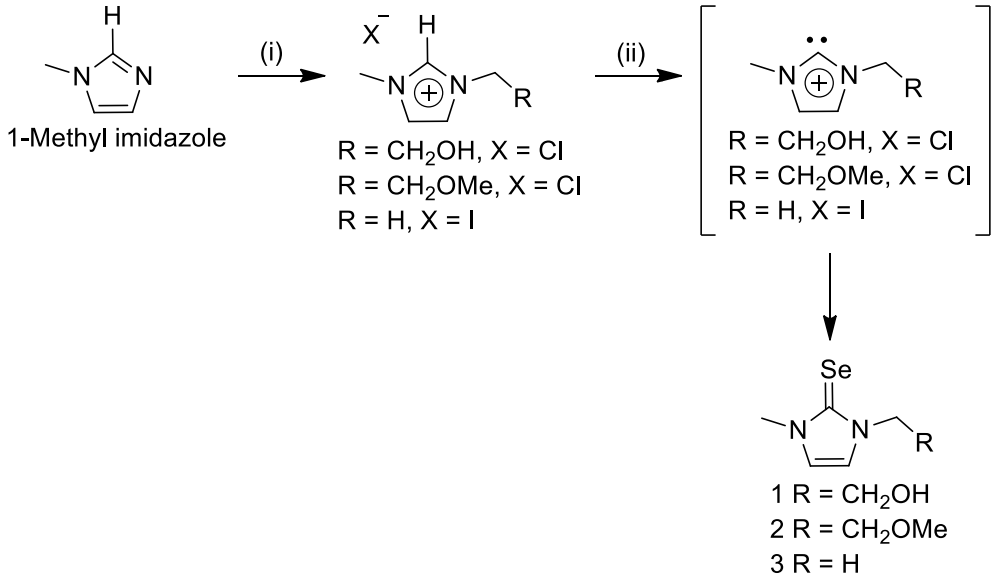

Scheme S1. Synthesis of *N,N'*-disubstituted selones by using heterocyclic carbenes generated *in situ* from the corresponding imidazolium salts. Reagents and conditions: (i) Chloroethanol, 80ºC (for $Im^{OH}Se$); 2-Chloroethyl methyl ether, 80ºC (for $Im^{OMe}Se$); CH_3I/ ethyl acetate, 2h, rt (for $Im^{Me}Se$)**;** (ii) K_2CO_3, dry methanol, Se powder, reflux, 12 h.

III. NMR Analyses:

A

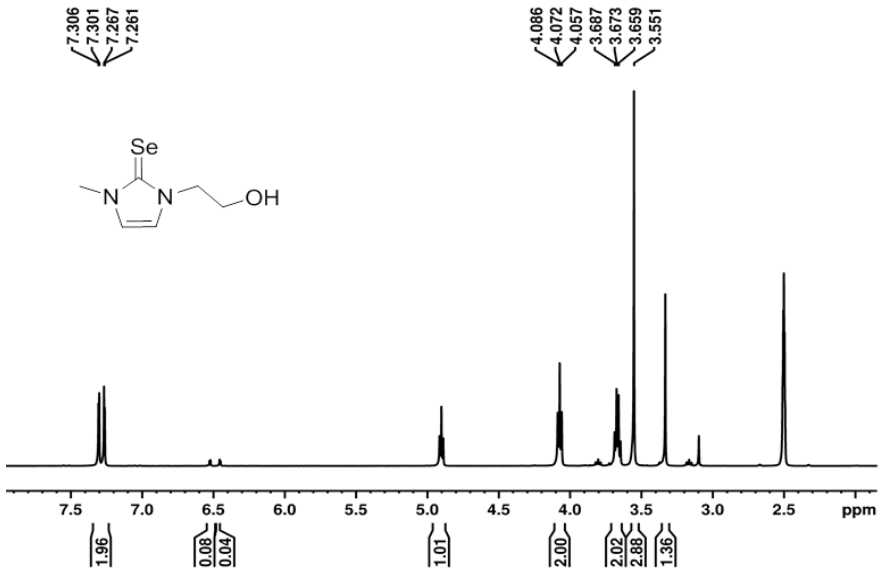

B

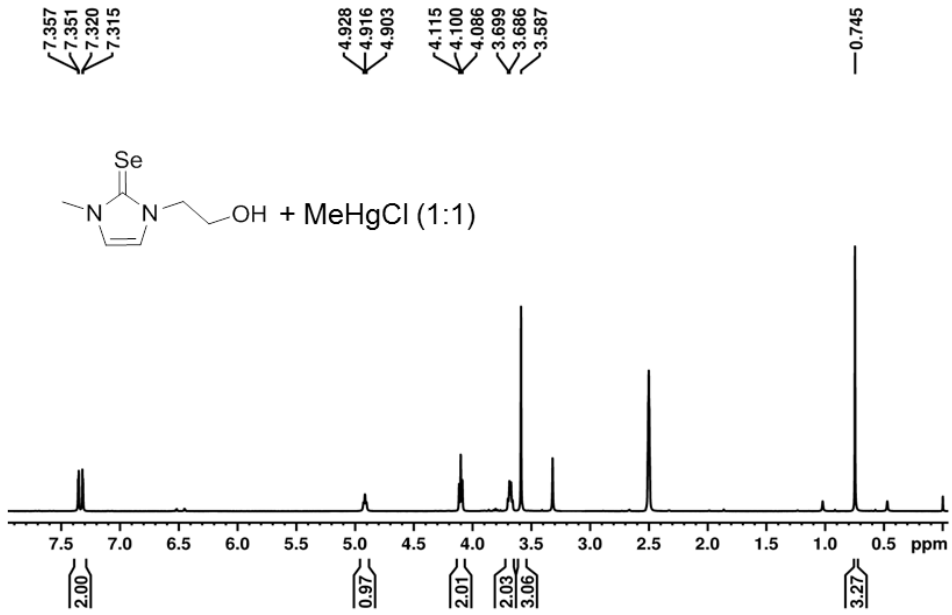

Figure S1: Comparison of ^{1}H NMR spectrum of Im^{OH}Se (A) with Im^{OH}Se/MeHgCl (1:1) (B) in DMSO-d_6 (down).

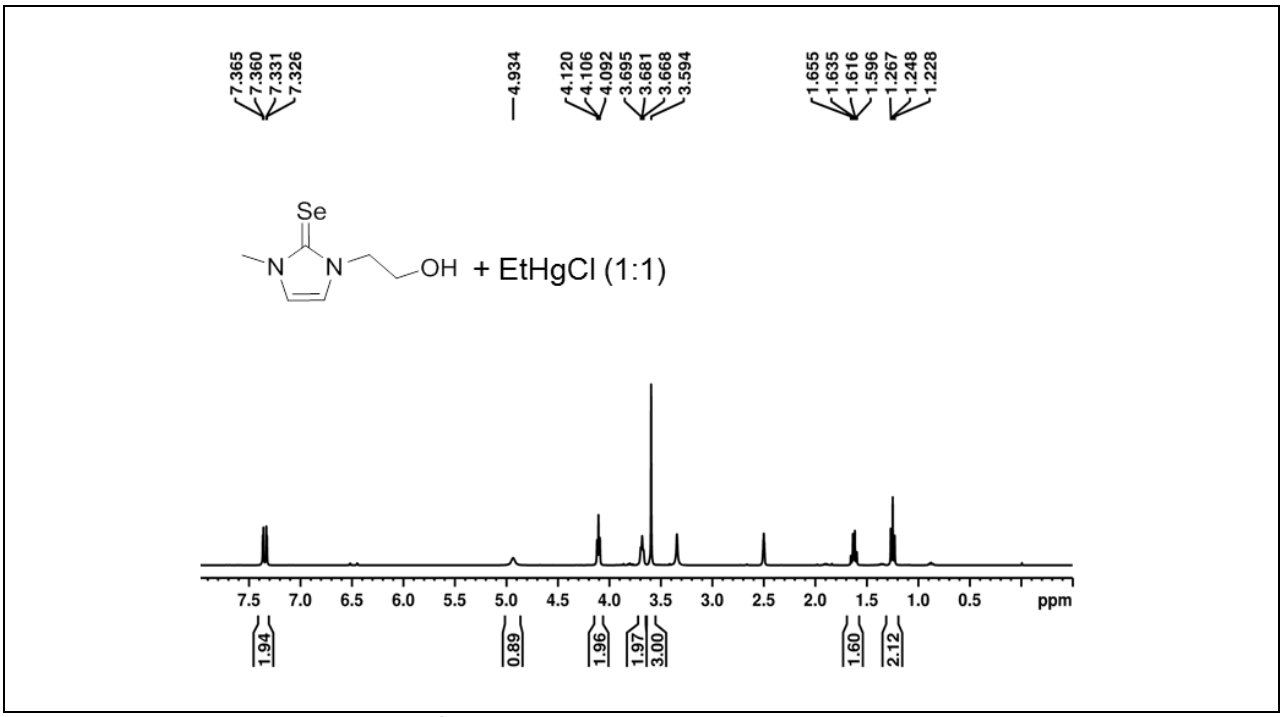

Figure S2: ^{1}H NMR spectrum of Im^{OH}Se/EtHgCl (1:1) in DMSO-d_6.

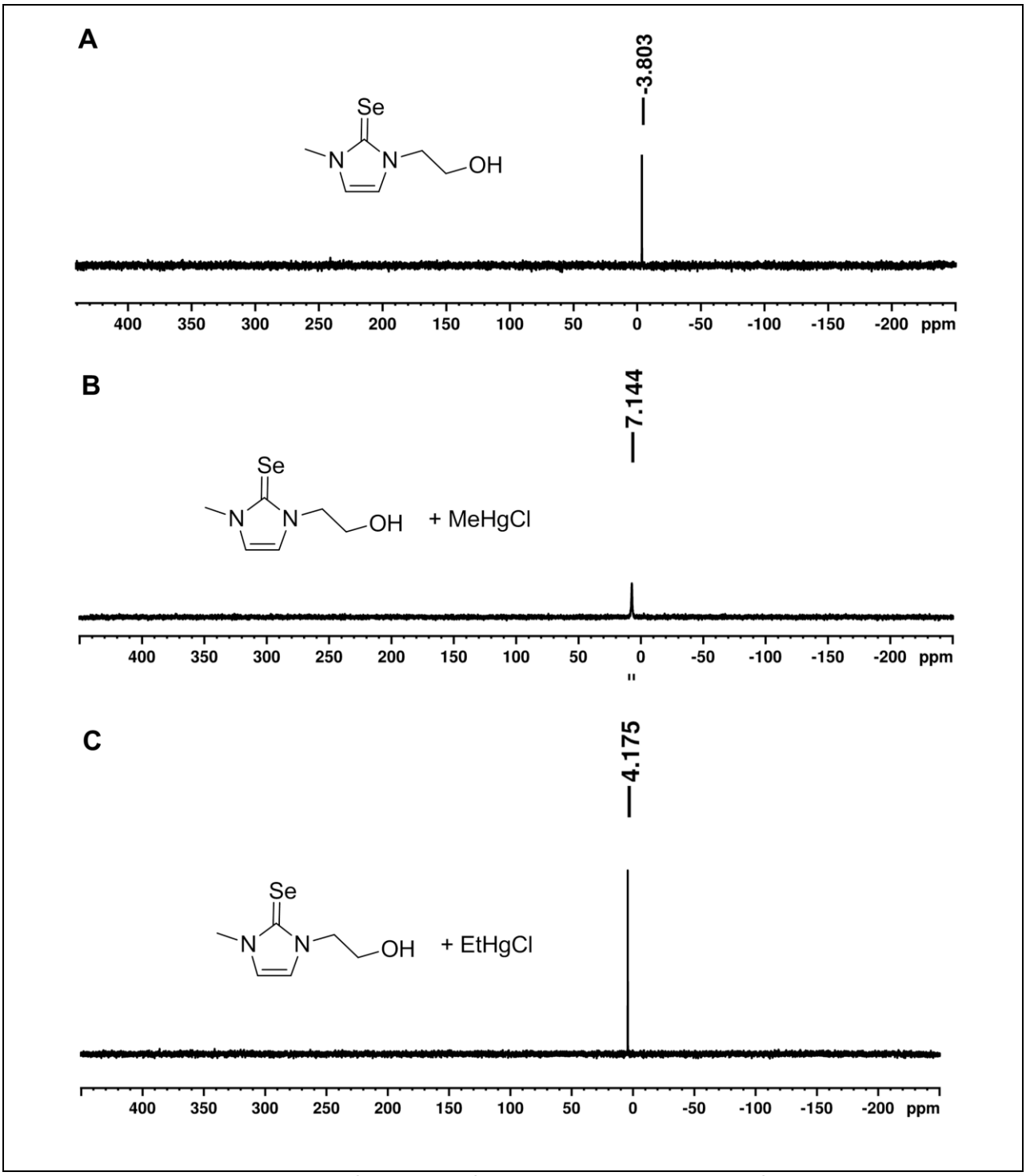

Figure S3: ^{77}Se NMR spectra of Im^{OH}Se (A), Im^{OH}Se/MeHgCl (1:1) (B) and Im^{OH}Se/EtHgCl (1:1) (C) in $CDCl_3$.

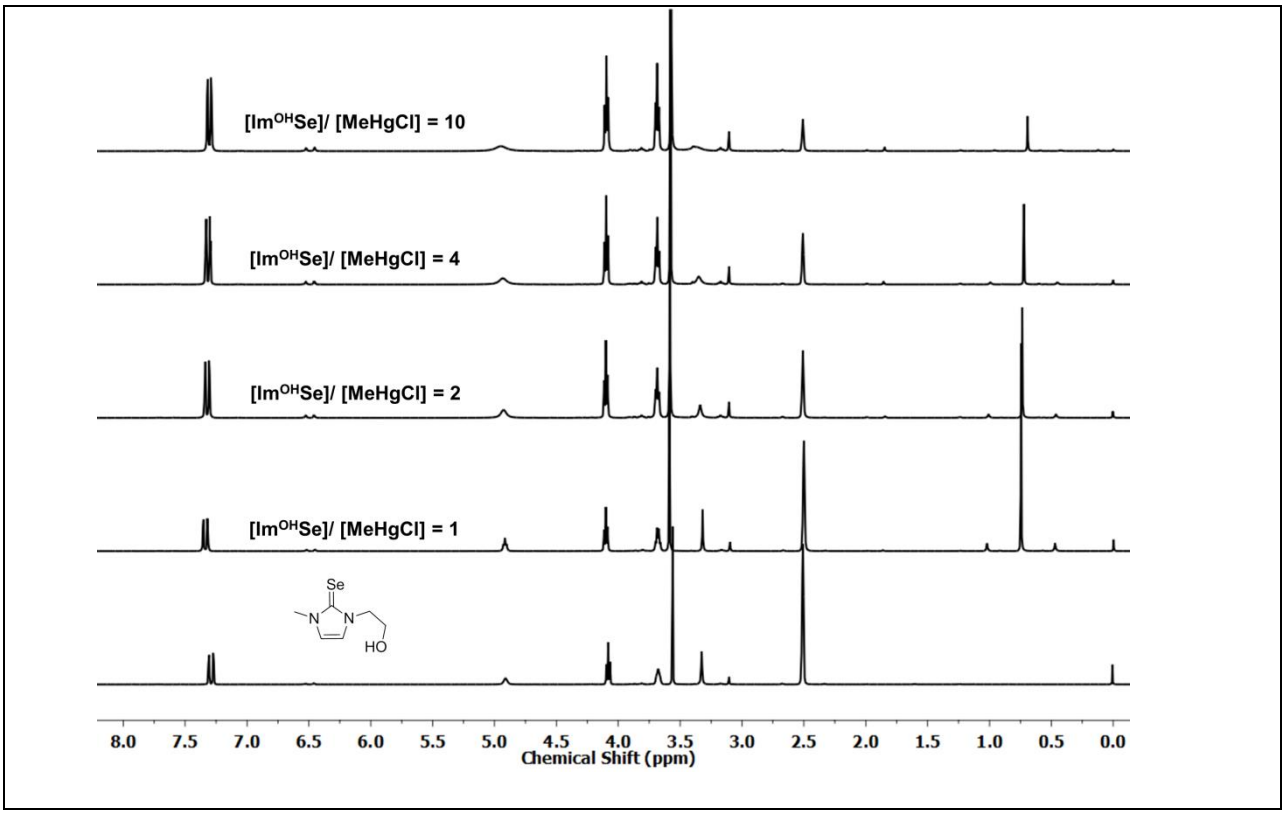

Figure S4: ^{1}H NMR spectra of Im^{OH}Se and the solution containing MeHgCl and various amounts of Im^{OH}Se (1 to 10 equivalents) in DMSO-d_6.

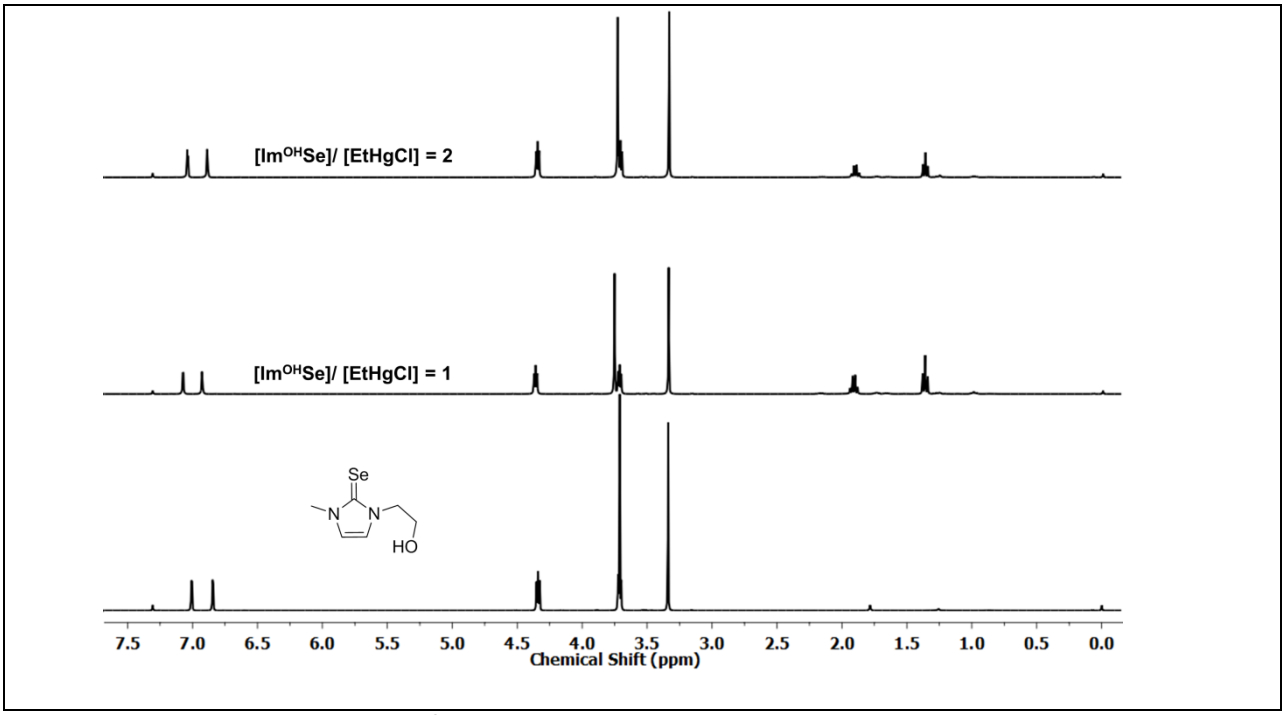

Figure S5: ^{1}H NMR spectra of Im^{OH}Se and the solution containing EtHgCl and various amounts of Im^{OH}Se (1 and 2 equivalents) in DMSO-d_6.

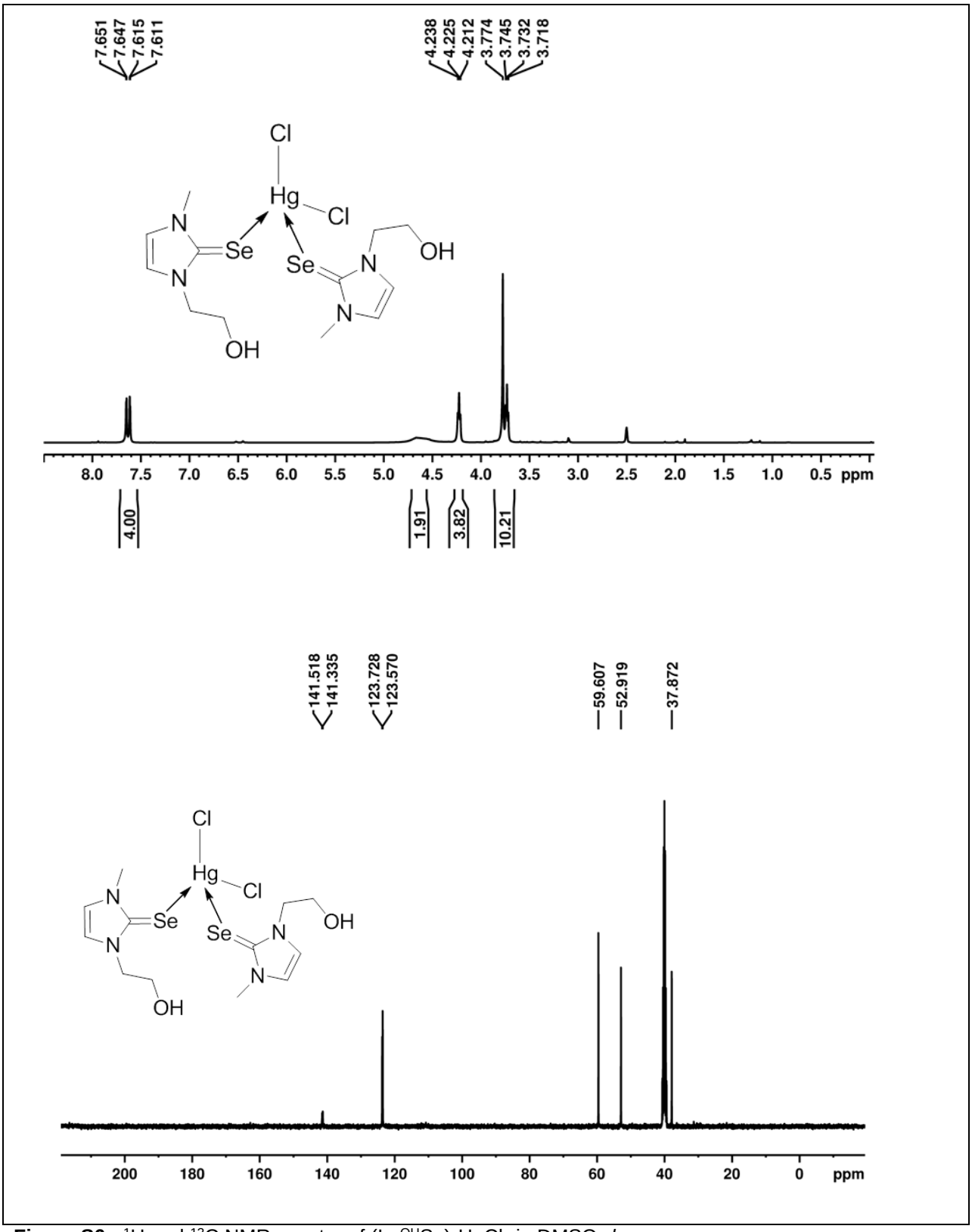

Figure S6: ^{1}H and ^{13}C NMR spectra of $(Im^{OH}Se)_2HgCl_2$ in DMSO-d_6.

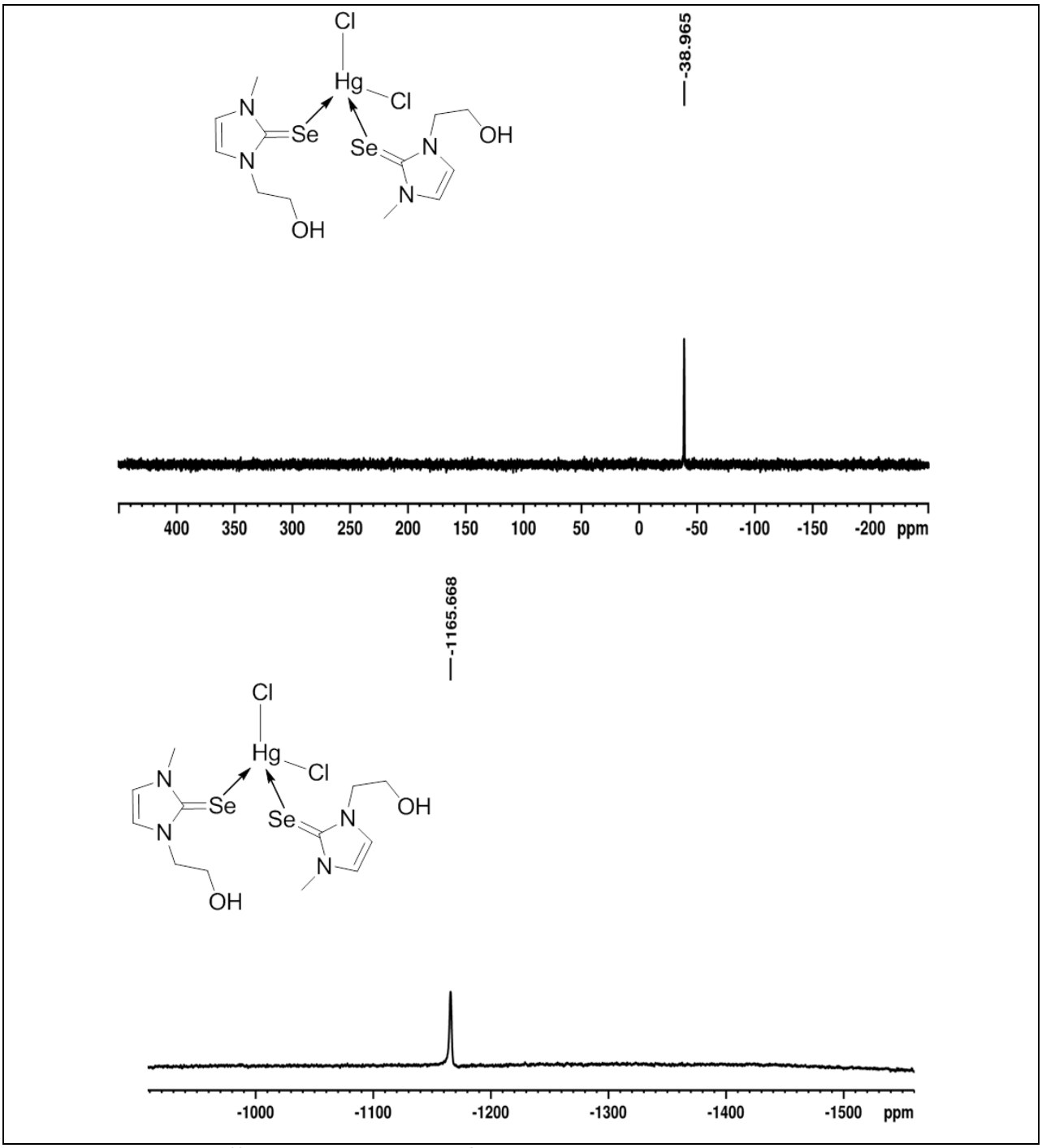

Figure S7: ^{77}Se and ^{199}Hg NMR spectra of $(Im^{OH}Se)_2HgCl_2$ in DMSO-d_6.

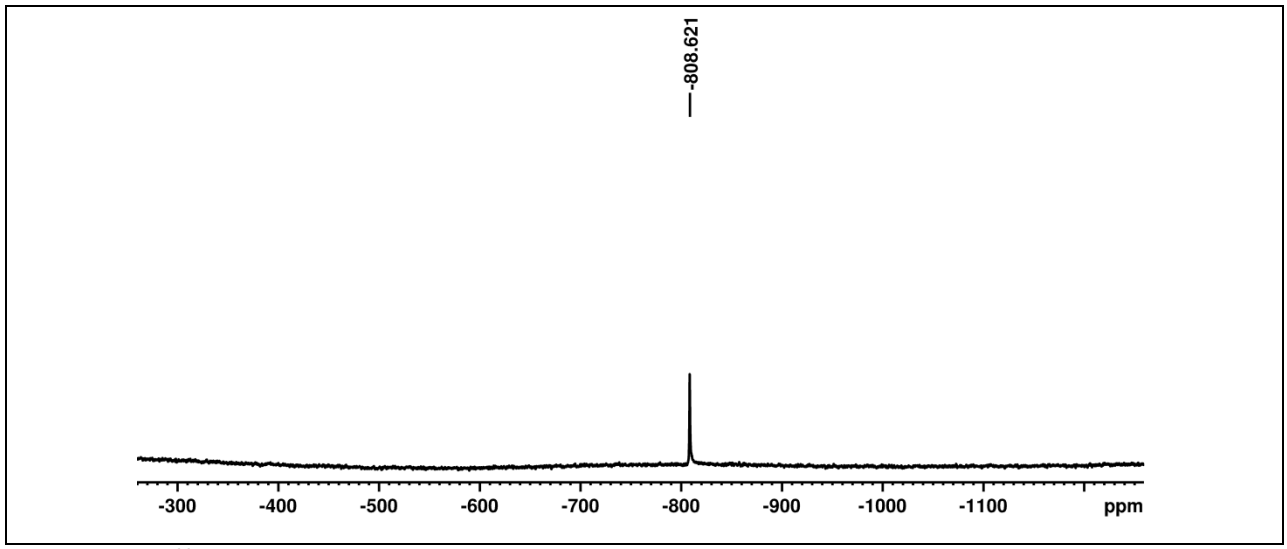

Figure S8: ^{199}Hg NMR spectrum of MeHgCl in $CDCl_3$.

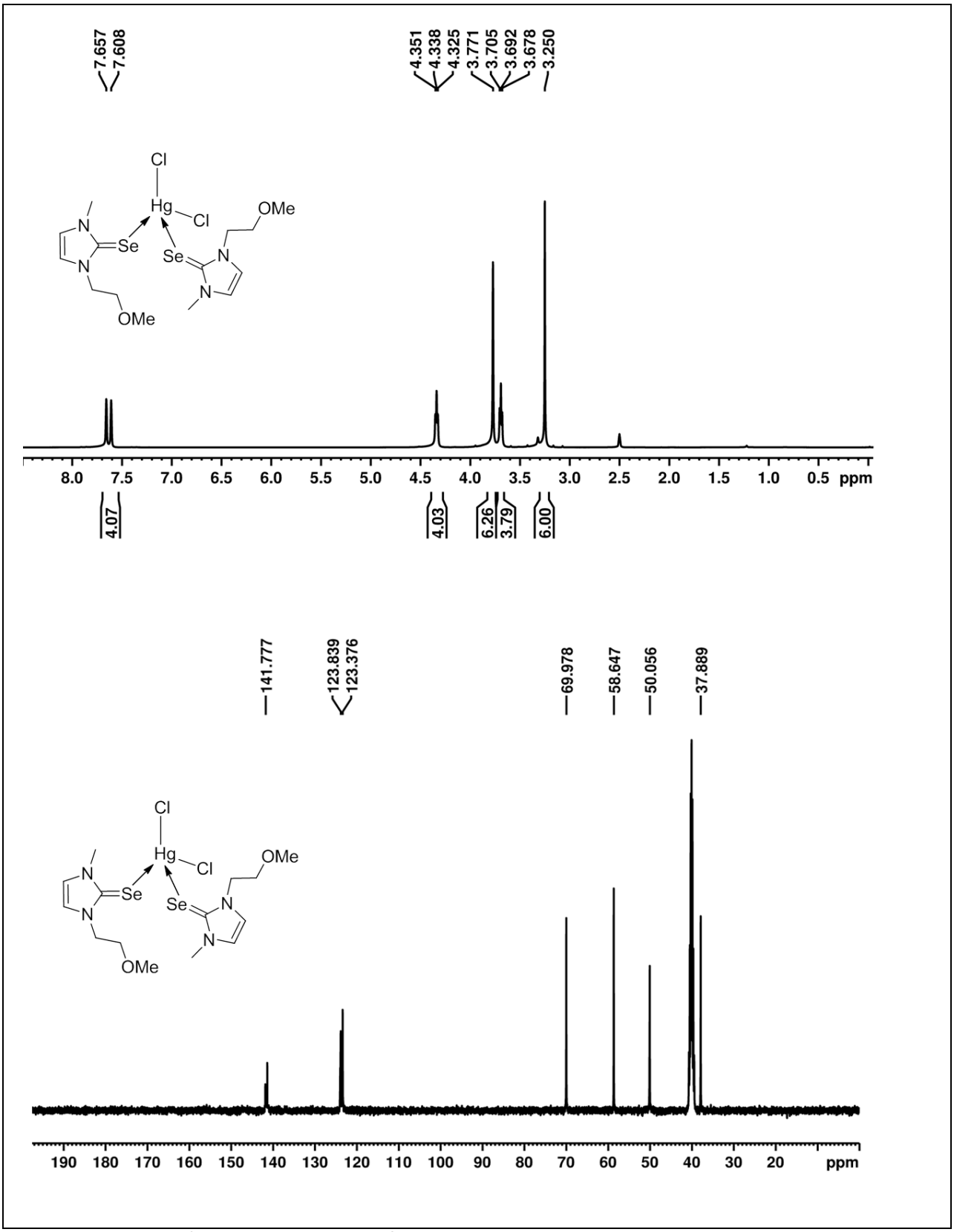

Figure S9: ^{1}H and ^{13}C NMR spectra of $(Im^{OMe}Se)_2HgCl_2$ in DMSO-d_6.

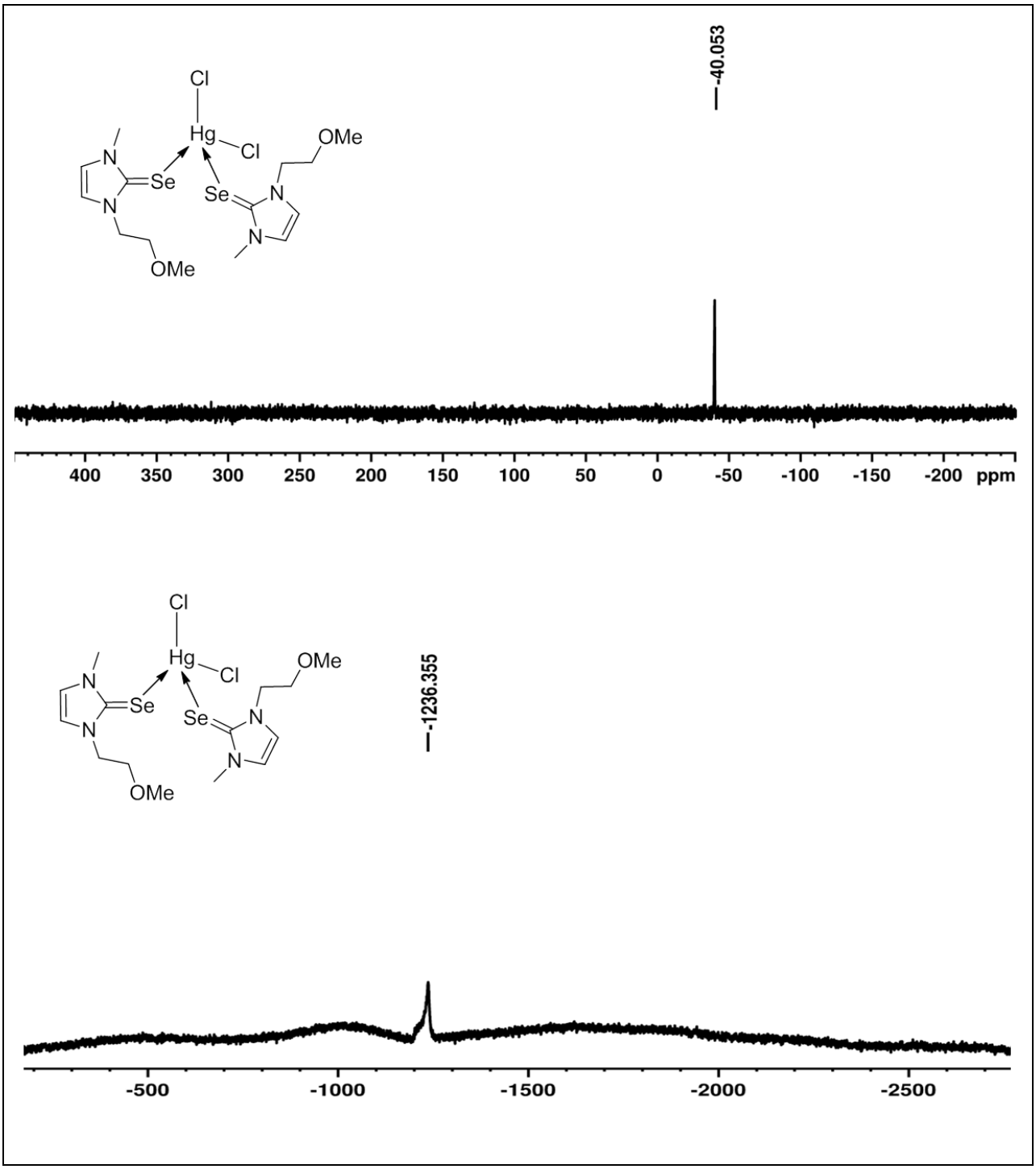

Figure S10: ^{77}Se and ^{199}Hg NMR spectra of $(Im^{OMe}SeHg)_2Cl_2$ in DMSO-d_6.

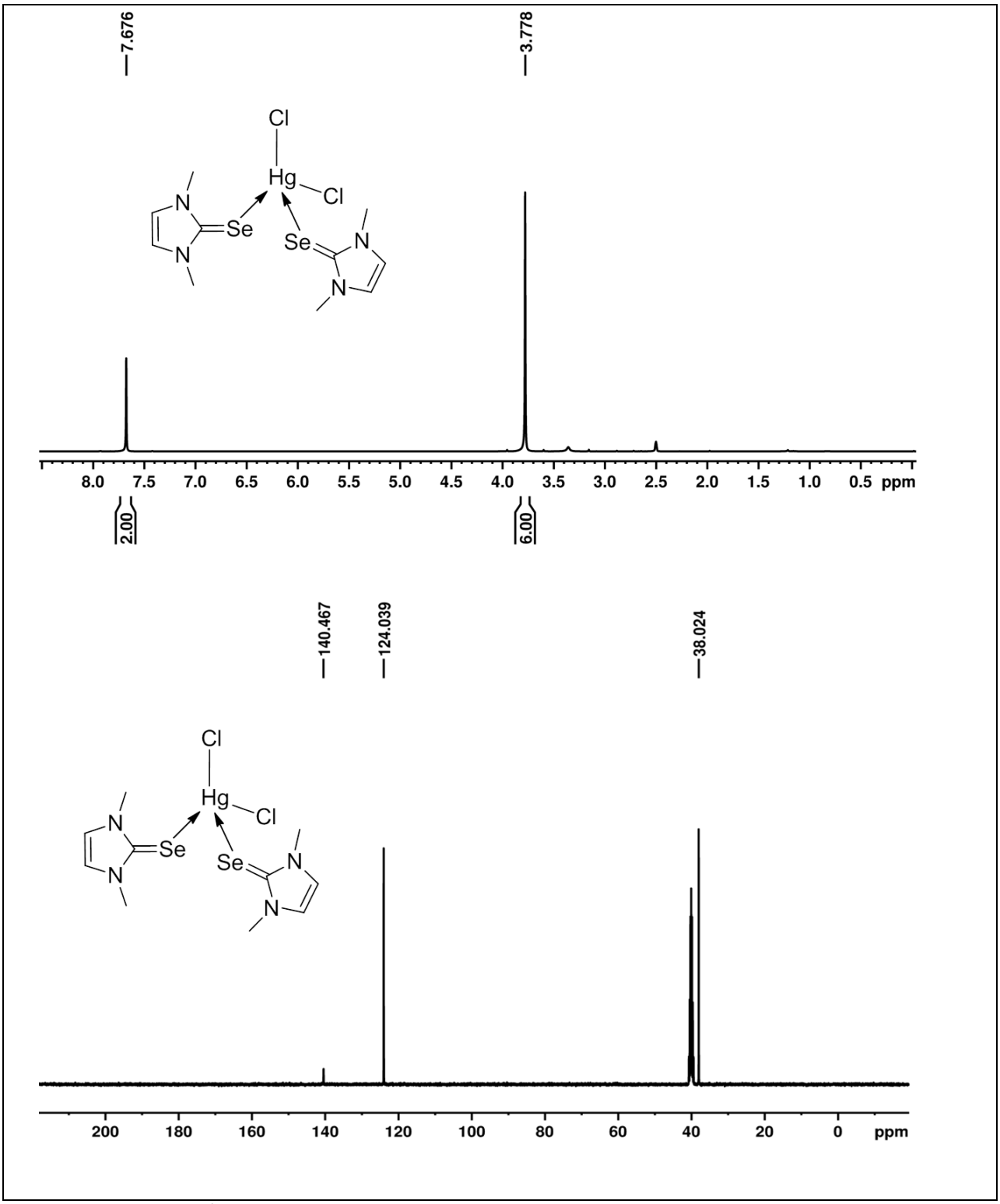

Figure S11: ^{1}H and ^{13}C NMR spectra of $(Im^{Me}Se)_2HgCl_2$ in DMSO-d_6.

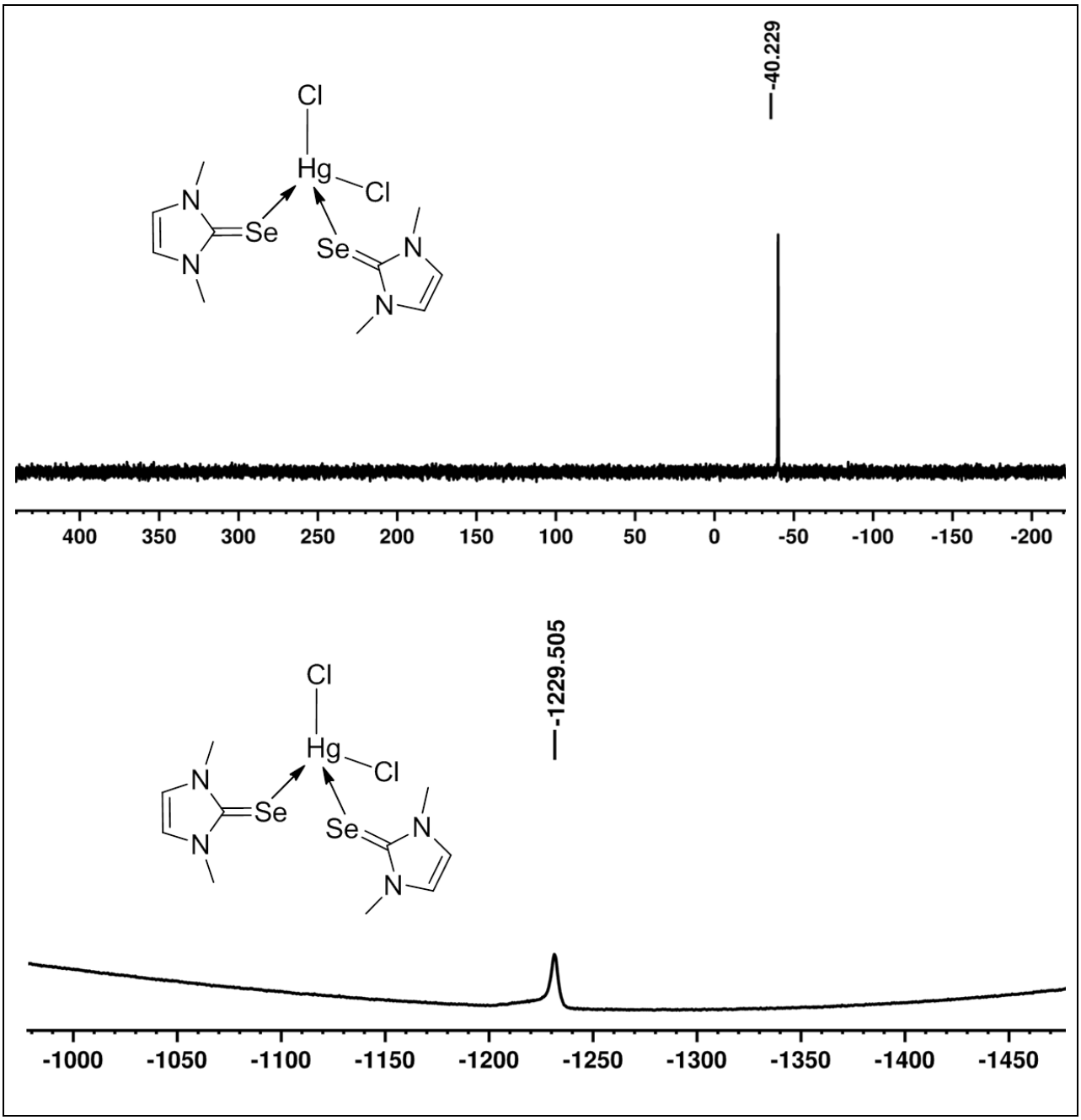

Figure S12: ^{77}Se and ^{199}Hg NMR spectra of $(Im^{Me}Se)_2HgCl_2$ in DMSO-d_6.

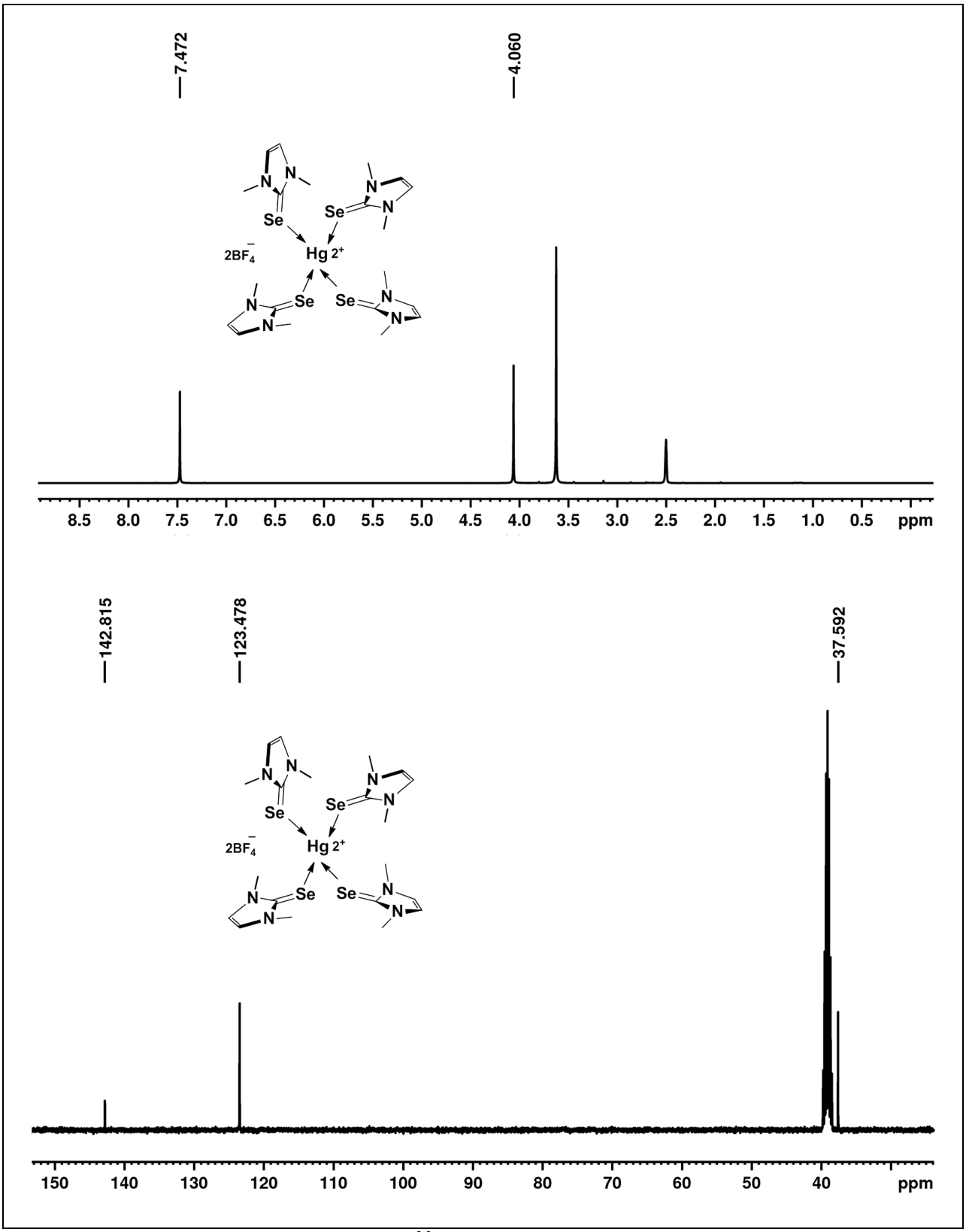

Figure S13: ^{1}H and ^{13}C NMR spectra of $[(Im^{Me}Se)_4Hg](BF_4)_2$ in DMSO-d_6.

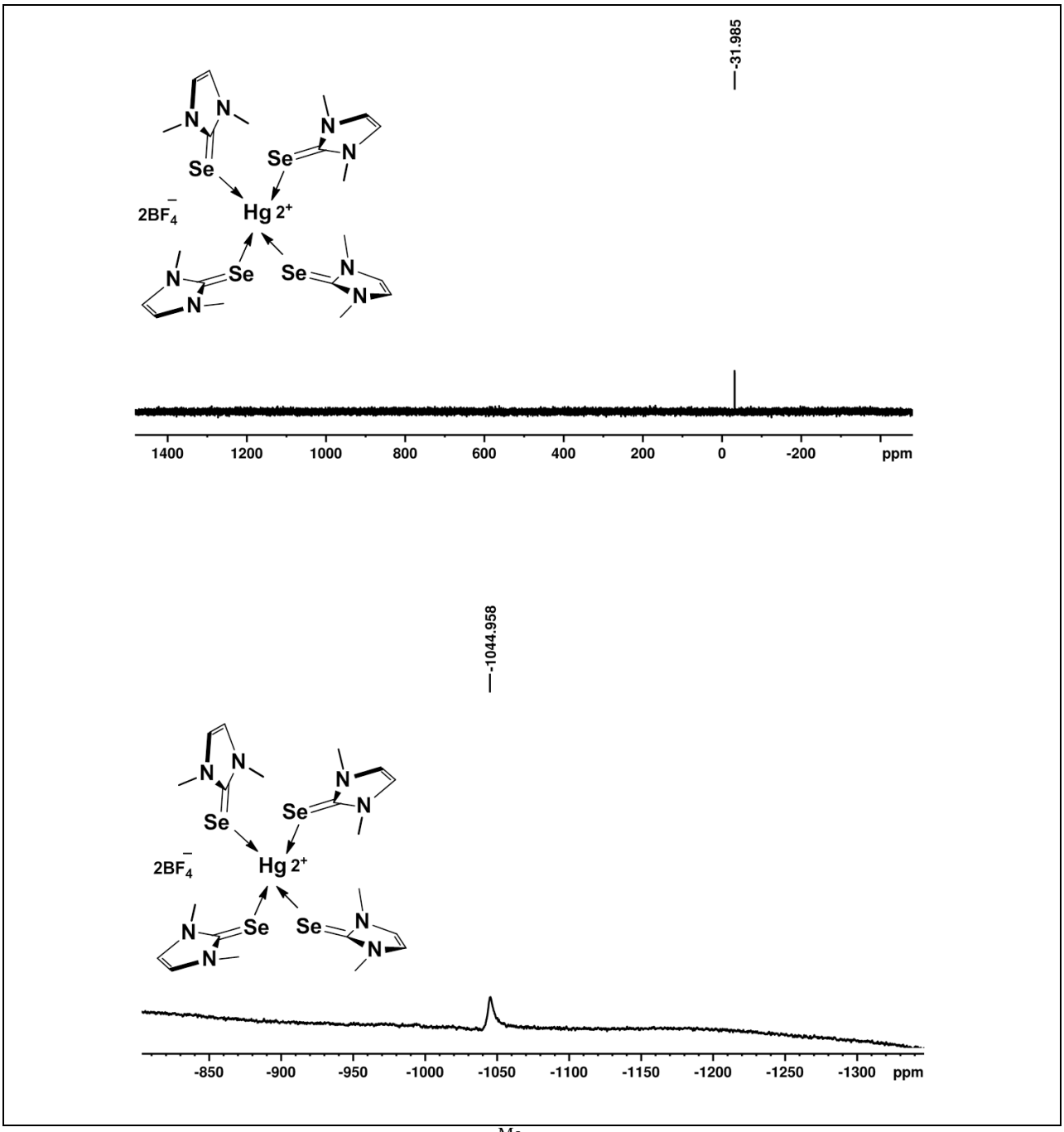

Figure S14: ^{77}Se and ^{199}Hg NMR spectra of $[(Im^{Me}Se)_4Hg](BF_4)_2$ in DMSO-d_6.

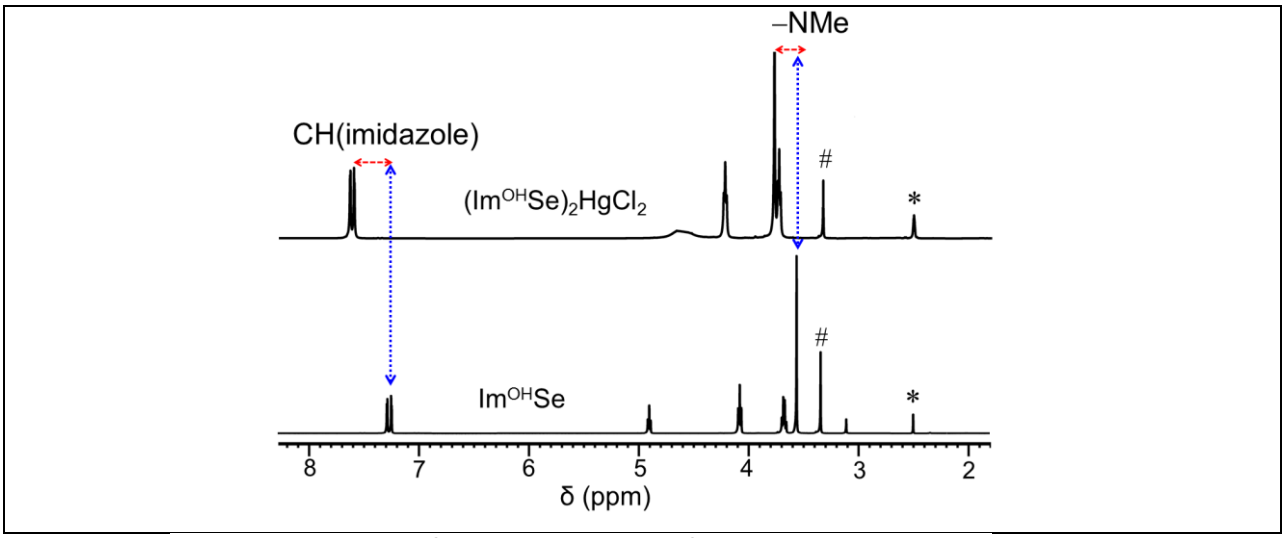

Figure S15: ^{1}H NMR spectra of $Im^{OH}Se$ and isolated $(Im^{OH}Se)_2HgCl_2$ in DMSO-d_6.

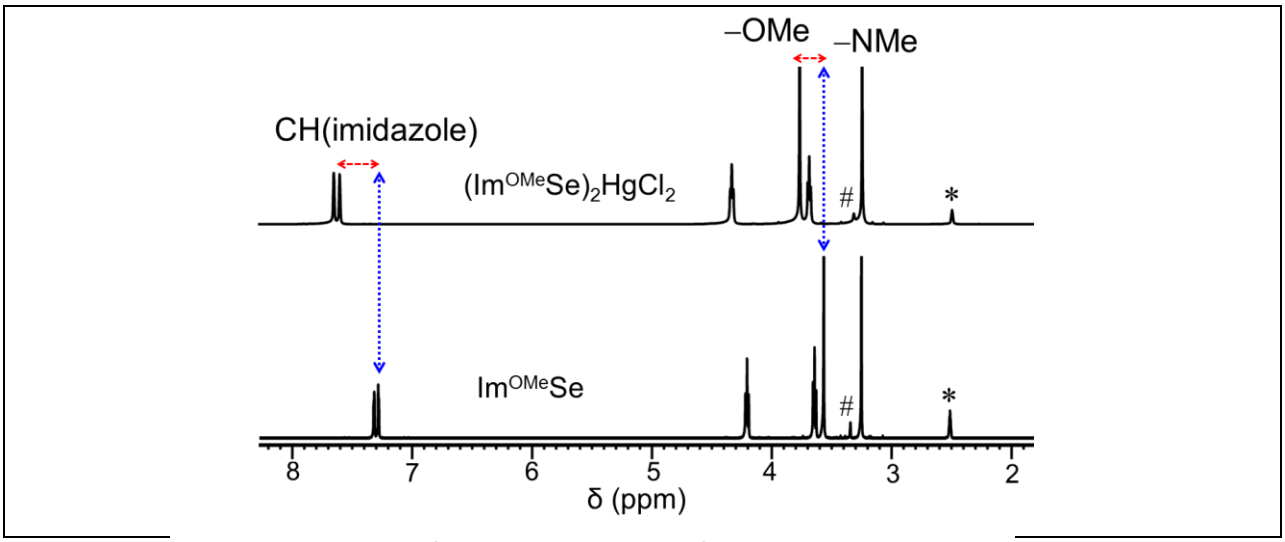

Figure S16: ^{1}H NMR spectra of $Im^{OMe}Se$ and isolated $(Im^{OMe}Se)_2HgCl_2$ in DMSO-d_6.

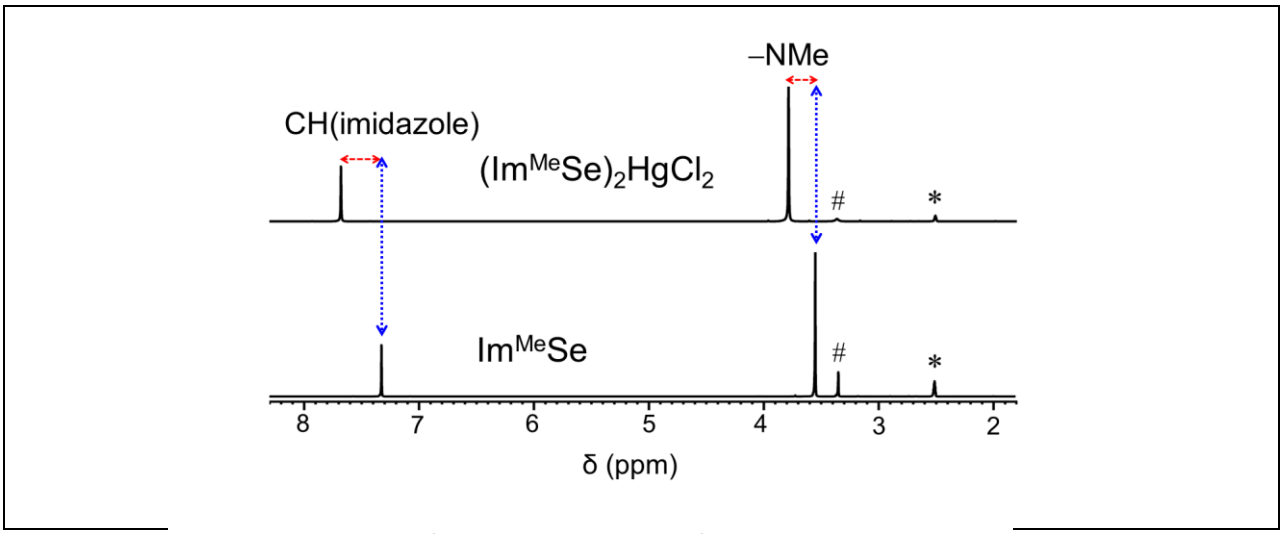

Figure S17: ^{1}H NMR spectra of Im^{OMe}Se and isolated (Im^{OMe}Se)$_2$HgCl$_2$ in DMSO-d$_6$.

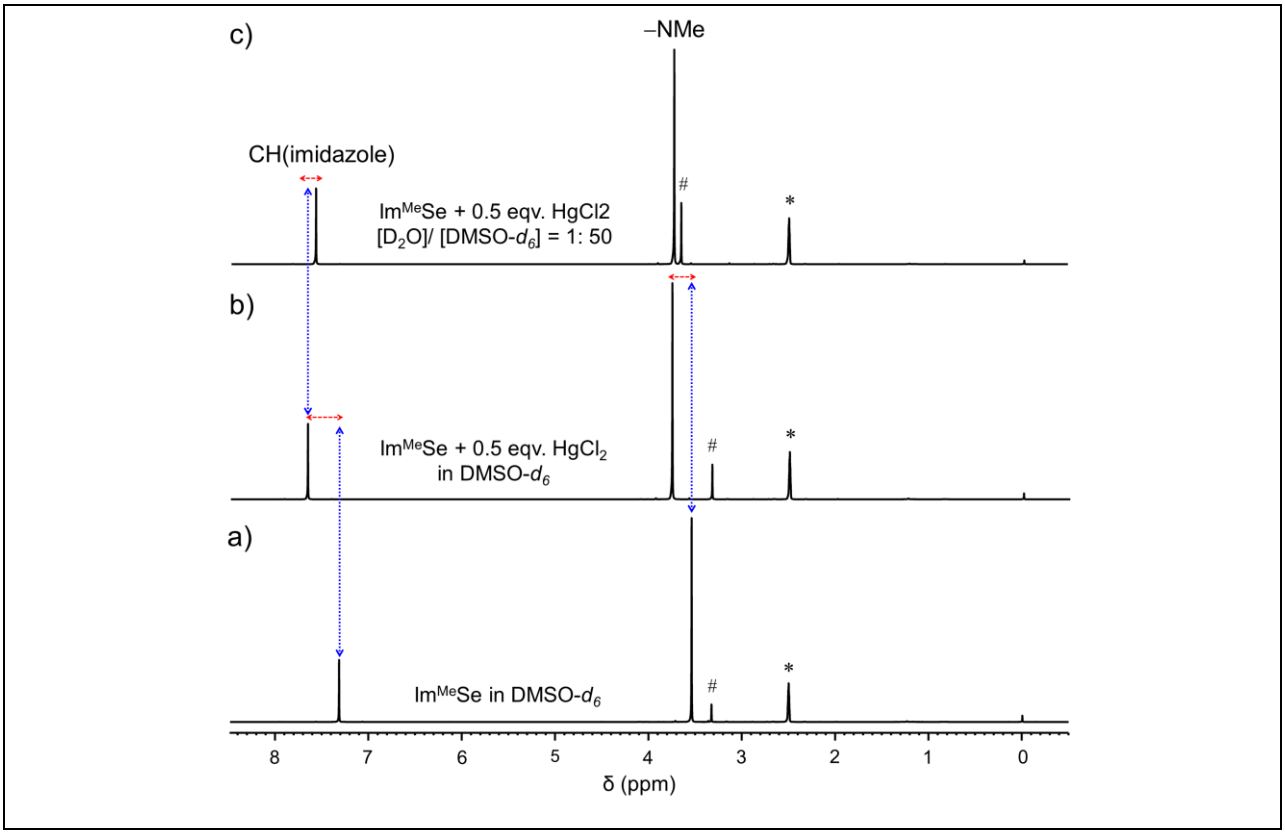

Figure S18: ^{1}H NMR spectra showing significant downfield shift (0.22 ppm) for olefinic -CH and significant downfield shift (0.33 ppm) for –NMe proton of Im^{Me}Se on coordination to HgCl$_2$ in DMSO-*d*$_6$ (* = solvent signal; # residual water signal) (a and b) but addition of D$_2$O results a minor up field shift for both olefinic –CH proton (0.06 ppm) and –NMe proton (0.02 ppm) (c).

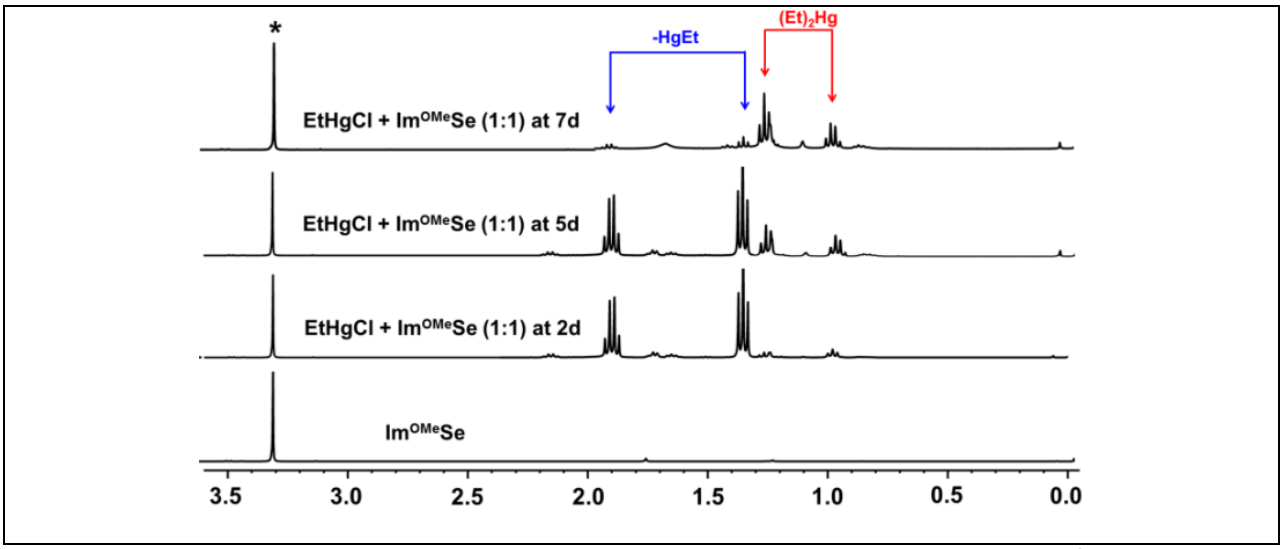

Figure S19: ^{1}H NMR spectra showing the formation of $(Et)_2Hg$ in the reaction between $Im^{OMe}Se$ and EtHgCl in 1:1 ratio in $CDCl_3$. (* = -NMe proton of $Im^{OMe}Se$)

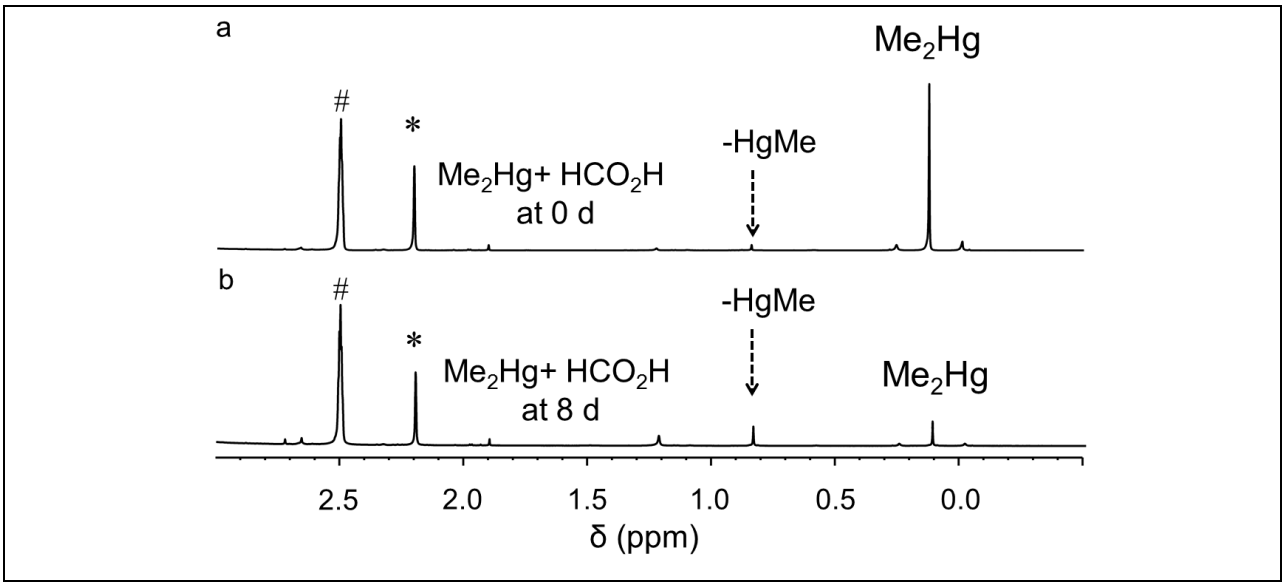

Figure S20: ^{1}H NMR spectra showing the degradation of $(Me)_2Hg$ in acidic medium. a) ^{1}H NMR spectrum in DMSO-d_6 of the reaction solution containing MeHgCl and $Im^{OH}Se$ in (1:1 ratio) at 2nd day, b) ^{1}H NMR spectrum of the above reaction mixture after addition of one equivalent of HCO_2H at 8 day. (∗ = mesitylene peak; # = solvent peak).

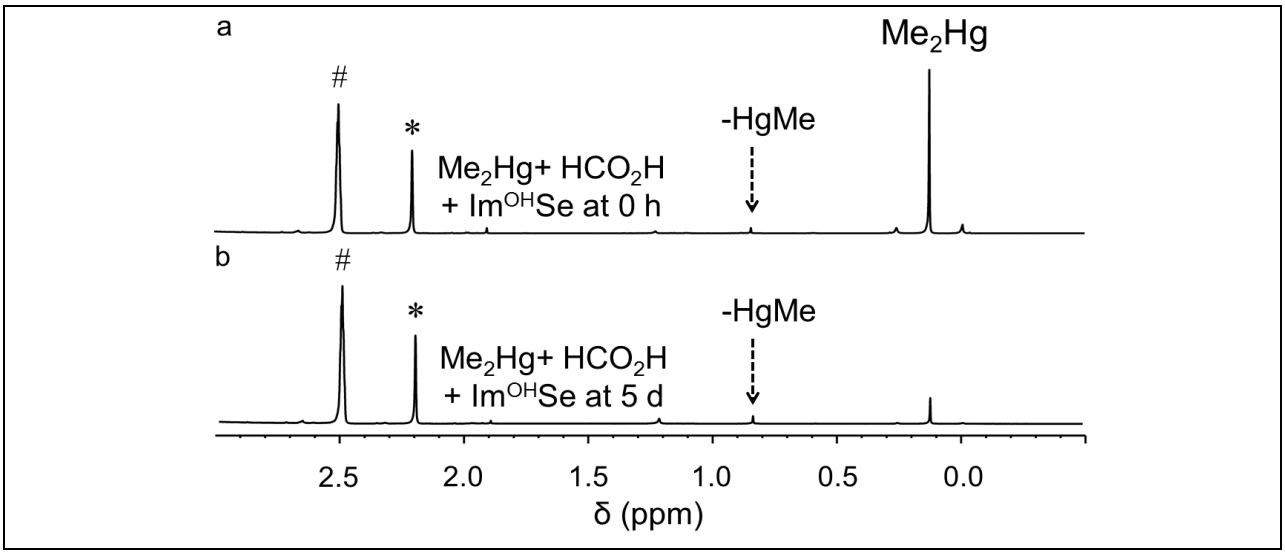

Figure S21: ^{1}H NMR spectra showing the degradation of $(Me)_2Hg$ in acidic medium. a) ^{1}H NMR spectrum in DMSO-d_6 of the reaction solution containing MeHgCl and $Im^{OH}Se$ in (1:1 ratio) at 2nd day, b) ^{1}H NMR spectrum of the above reaction mixture after addition of one equivalent of HCO_2H (FA) and four equivalents of $Im^{OH}Se$ at 7day. (∗ = mesitylene peak; # = solvent peak).

IV. X-ray Crystallography Analyses:

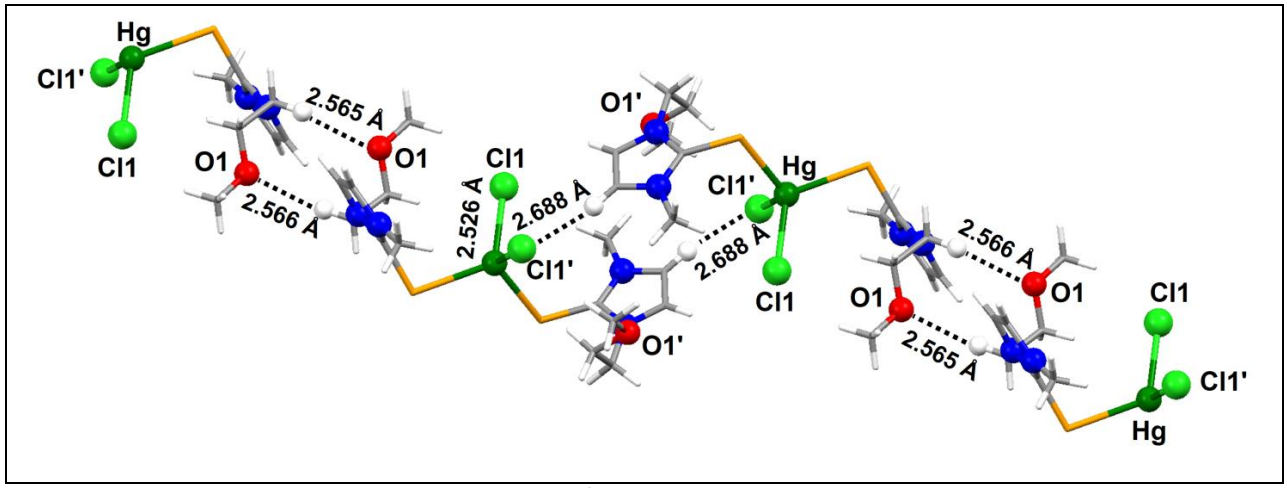

Figure S22. Crystal packing diagram of $(Im^{OMe}Se)_2HgCl_2$ showing a trimeric structure due several intermolecular interactions.

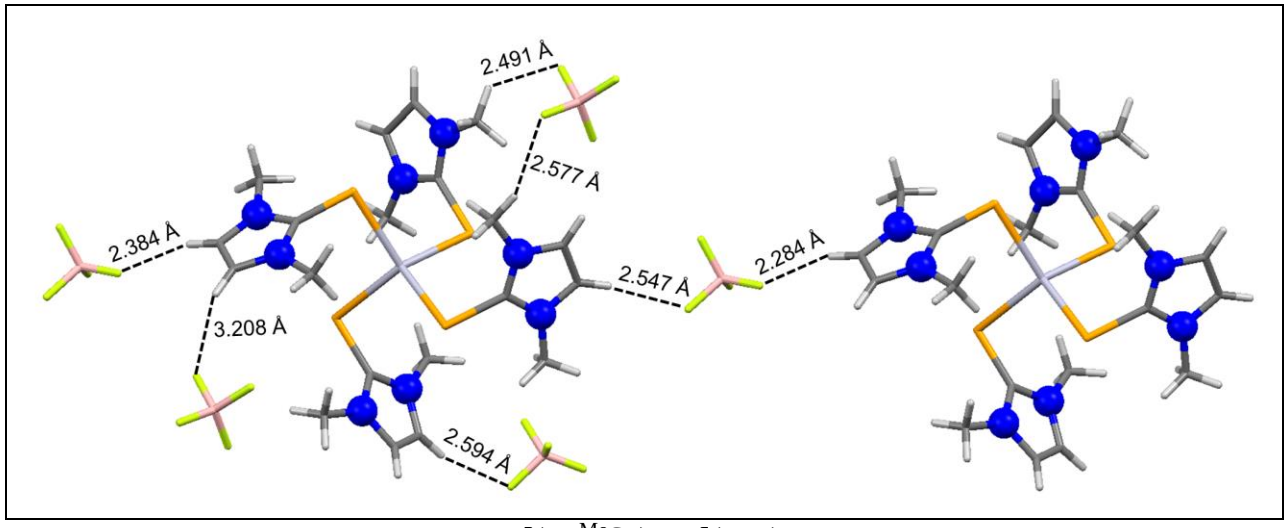

Figure S23. Crystal packing diagram of $[(Im^{Me}Se)_4Hg](BF_4)_2$ showing nonbonded intermolecular C-H….F interactions.

Table S1. Crystallographic data for compounds $(Im^{OMe}Se)_2HgCl_2$ and $(Im^{Me}Se)_2HgCl_2$.

	$(Im^{OMe}Se)_2HgCl_2$	$(Im^{Me}Se)_2HgCl_2$	$[(Im^{Me}Se)_4Hg](BF_4)_2$
	CCDC1541412	CCDC1541411	CCDC 1567515
Lattice	Monoclinic	Triclinic	Orthorhomic
Formula	$C_{14}H_{24}HgCl_2N_4O_2Se_2$	$C_{10}H_{16}Cl_2HgN_4Se_2$	$C_{20}H_{32}B2F_8HgN_8Se_4$
Formula Weight	709.78	621.68	1079.92
Space Group	C2/c	P_{-1}	$C_{ca2/1}$
a/ A°	15.7760(7)	8.2244(13)	21.7617 (7)
b/ A°	10.2117(5)	9.2192(15)	11.9671 (3)
c/ A°	15.1296(6)	13.5693(21)	13.3839 (4)
α/ °	90	93.529(6)	90
β/ °	116.207(2)	107.254(6)	90
γ/ °	90	116.255(5)	90
V/ $A^{\circ 3}$	2186.82(17)	858.58(40)	3845.49 (18)
Z	6	2	4
Temperature (K)	297	298	298
Radiation (λ)/A°	0.71073	0.71073	0.71073
ρ/ (g cm^{-3})	2.156	2.405	2.058
μ (Mo K_α) mm^{-1}	13.203	13.506	8.661
θ_{max}/deg	26.4	25.7	24.6
No. of data collected	2255	3519	63319
No. of data	1979	3162	7122
No. of parameters	117	177	397
R_1 [I> 2σI]	0.024	0.017	0.037
wR_2 [I> 2σI]	0.050	0.035	0.078
R_1 [all data]	0.033	0.023	0.080
wR_2 [all data]	0.053	0.035	0.096
R_{int} [all data]	0.0482	0.0441	0.096
GOF	1.026	1.068	0.926

Table S2. Selected bond lengths and bond angles of $(Im^{Me}Se)_2HgCl_2$

Bond lengths (Å)		Bond angles (Å)	
Hg-Se1	2.5990(6)	Se1- Hg- Se1'	126.15
Hg-Se2	2.5903(5)	Se1- Hg- Cl2	103.24
Se1-C2	1.880(2)	Se1- Hg- Cl1	109.58
Se1'-C2'	1.867(2)	Se1'- Hg- Cl2	104.52
Hg-Cl1	2.5621(8)	Se1'- Hg- Cl1	105.57
Hg-Cl2	2.558(1)	Cl2- Hg- Cl1	105.77

Table S3. Selected bond lengths and bond angles of $(Im^{OMe}Se)_2HgCl_2$

Bond lengths (Å)		Bond angles (Å)	
Hg-Se1 = Hg-Se1'	2.6079(5)	Se1- Hg Cl1	115.52
Se1-C2 = Se1'-C2'	1.868(3)	Se1- Hg- Cl1'	108.83
Hg-Cl1 = Hg-Cl1'	2.525(9)	Se1- Hg- Se1'	107.45
		Cl1- Hg- Cl1'	100.88

Table S4. Selected bond lengths and bond angles of $[(Im^{Me}Se)_4Hg](BF_4)_2$

Bond lengths (Å)		Bond angles (°)	
Hg-Se1	2.660(4)	Se1- Hg- Se2	106.22
Hg-Se2	2.618(5)	Se2- Hg- Se3	103.32
Hg-Se3	2.639(4)	Se3- Hg- Se4	105.80
Hg-Se4	2.607(4)	Se4- Hg- Se1	102.87
C1-Se1	1.880(2)	Se1- Hg- Se3	115.06
C2-Se2	1.795(3)	Se2- Hg- Se4	124.20
C3-Se3	1.843(2)		
C41-Se4	1.895(2)		

V. HRMS Analyses:

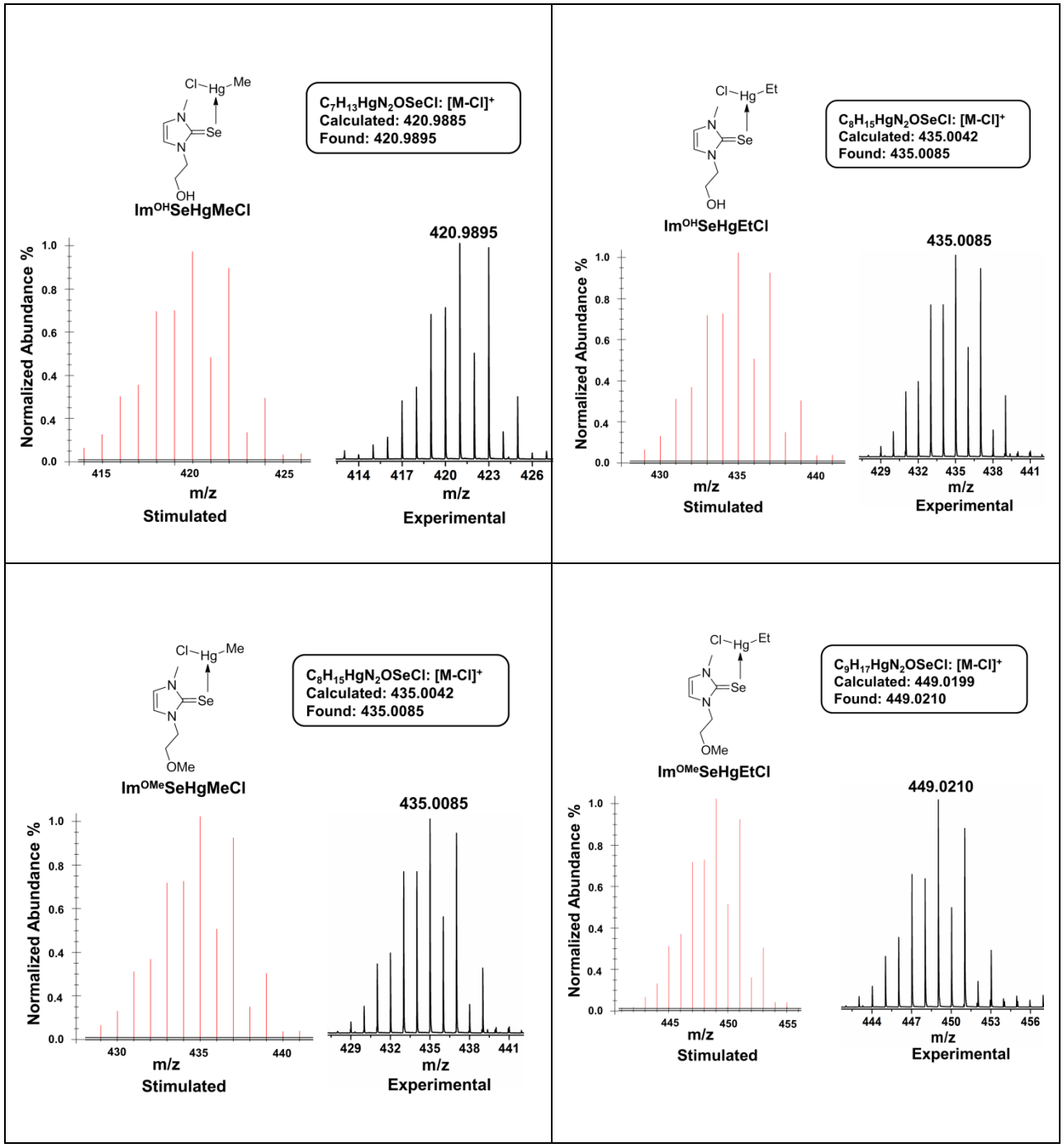

Figure S24. HRMS values of the 1:1RHg-conjugated complexes formed in the reaction between RHgCl (R = Me, Et) and $Im^{Y}Se$ (Y = OH, OMe) .

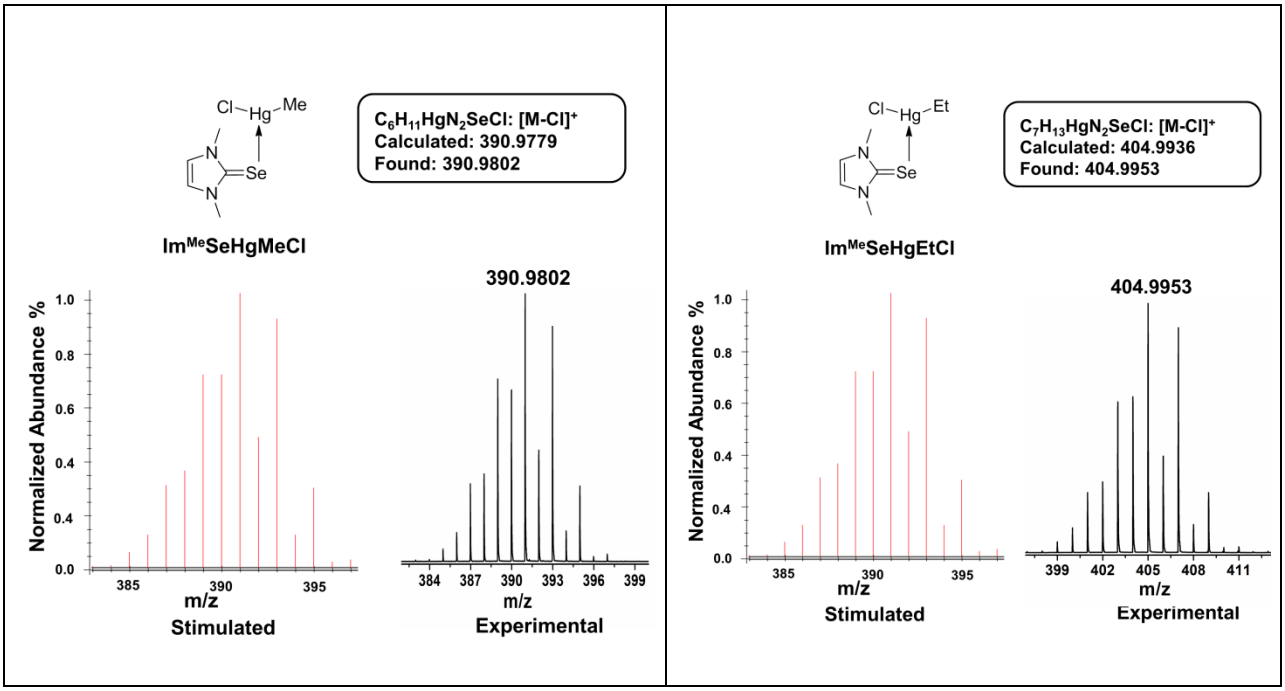

Figure S25. HRMS values of the 1:1RHg-conjugated complexes formed in the reaction between RHgCl (R = Me, Et) and $Im^{Me}Se$.

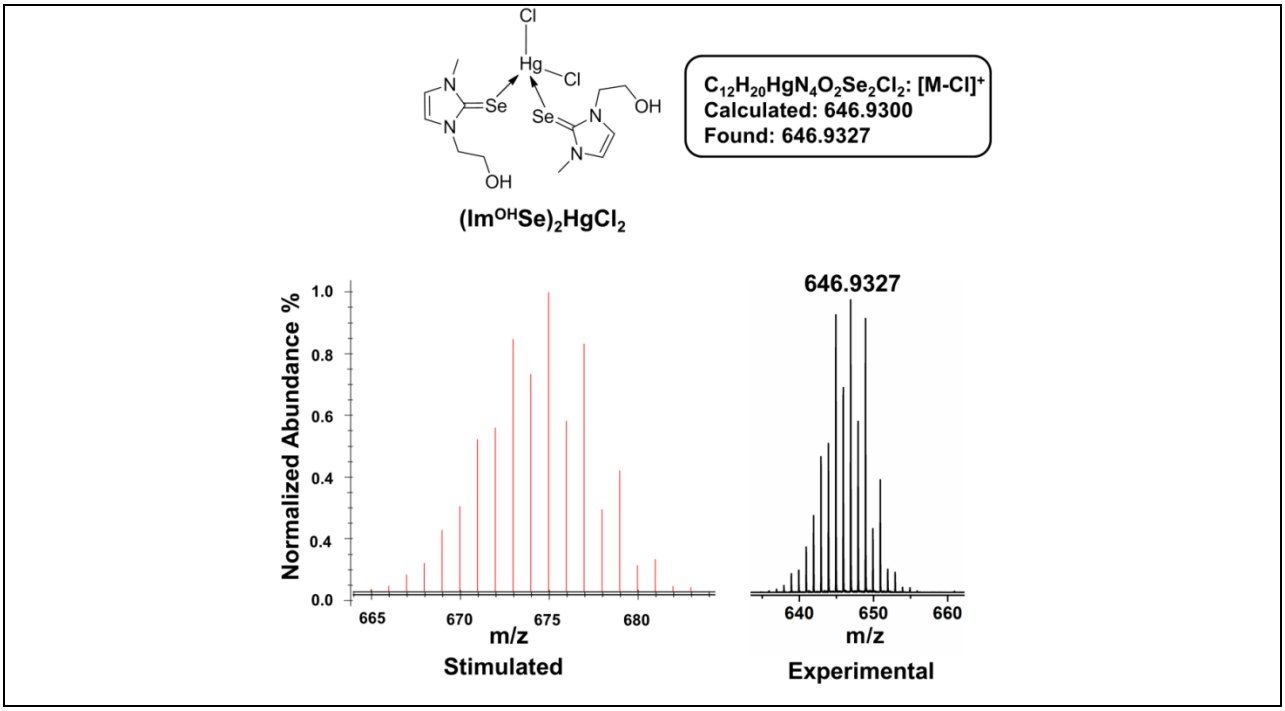

Figure S26. HRMS of $(Im^{OH}se)_2HgCl_2$ isolated from the reaction between RHgCl (R = Me, Et) and $Im^{OH}Se$.

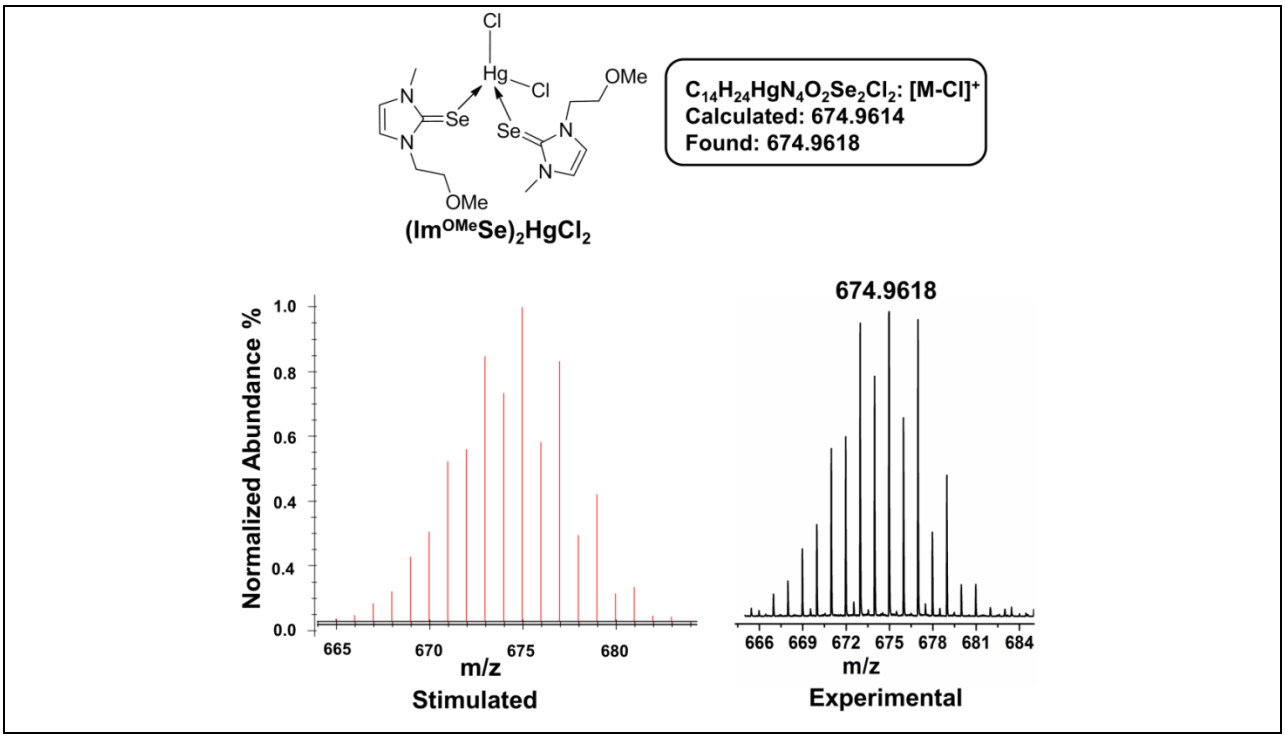

Figure S27. HRMS of $(Im^{OMe}se)_2HgCl_2$ isolated from the reaction between RHgCl (R = Me, Et) and $Im^{OMe}Se$.

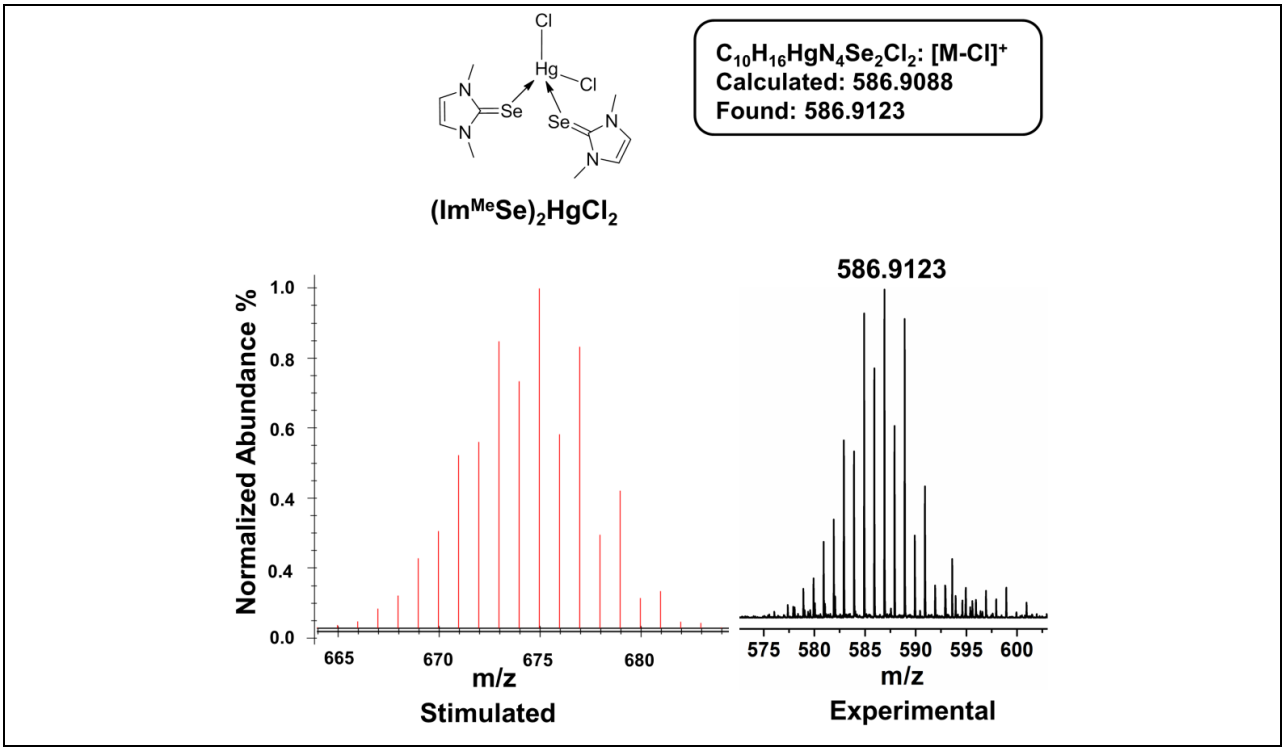

Figure S28. HRMS of $(Im^{Me}se)_2HgCl_2$ isolated from the reaction between RHgCl (R = Me, Et) and $Im^{Me}Se$.

VI. Preparation of water-soluble (HgSeS) nanoparticles from MeHgCys and MeHgSG:

General procedure for the degradation of MeHgCys by $Im^{OH}Se$. Compound $Im^{OH}Se$ (18.5 mg, 90 μmol) was added to the solution of MeHgX (X = Cys, SG; 90 μmol) in 3 ml of PBS buffer (pH 8.5) and stirred the reaction mixture (30 mM) at 37°C. The clear solution was gradually turned black after 6 h. An aliquot of 5 μl was taken from the above reaction mixture at various times and then diluted to 1 mL volume for HPLC analysis. Mobile phase: water/acetonitrile gradient. After completion of reaction, the black water-soluble Hg(SeS) nanoparticles were isolated by centrifugation and washed intensively with water and followed by with acetonitrile. Hg(SeS) powder were dried completely over vacuum and characterized thoroughly by various techniques such as SEM, TEM and EDX and IR analysis.

Synthesis of MeHgCys : To a solution of L-cysteine.HCl (100 mg, 0.56 mmol) in 10 ml of water/acetonitrile mixture (1:1), MeHgCl (140.6 mg, 0.56 mmol) was added and stirred overnight at 37°. After 10 h stirring white precipitate obtained was washed thoroughly with water and acetonitrile mixture to yield white solid powder, which was used for further studies.

Synthesis of MeHgSG : To a solution of L-glutathione (100 mg, 0.32 mmol) in 5 ml of water/acetonitrile mixture (1:1), MeHgCl (140.6 mg, 0.32 mmol) was added and stirred overnight at 37°. After 10 h stirring white precipitate obtained was washed thoroughly with water and acetonitrile mixture to yield white solid powder, which was used for further thiol exchange studies.

Synthesis of water-soluble HgSe nanoparticles in the reaction of MeHgCys/$Im^{OH}Se$:

A mixture of MeHgCys (30.4 mg, 0.09 mmol, 30 mM) and $Im^{OH}Se$ (18.5 mg, 0.09 mmol) was dissolved in 3 mL of either water/acetonitrile mixture (1:1) or phosphate buffer (pH 8.5) and stirred at 37°C. In case of water/acetonitrile mixture 2 equivalents of weak base $NaHCO_3$ or K_2HPO_4 was added after 1 h of stirring. After completion of reaction, the black precipitate of (HgSeS) was isolated by centrifugation and washed intensively with water and acetonitrile mixture and characterized thoroughly by various techniques such as SEM, TEM and EDX analysis (mentioned in article). Yield: 9 mg

Synthesis of water-soluble Hg(SeS) nanoparticles in the reaction of MeHgSG/ $Im^{OH}Se$:

A mixture of MeHgSG (46.9 mg, 0.09 mmol, 30 mM) and $Im^{OH}Se$ (18.5 mg, 0.09 mmol) was dissolved in 3 mL of either water/acetonitrile mixture (1:1) or phosphate buffer (pH 8.5) and stirred at 37°C. In case of water/acetonitrile mixture 2 equivalents of weak base $NaHCO_3$ or K_2HPO_4 was added after 1 h of stirring. After completion of reaction, the black precipitate of HgS was isolated by centrifugation and washed intensively with water and acetonitrile mixture and characterized thoroughly by various techniques such as SEM, TEM and EDX analysis. Yield: 12 mg

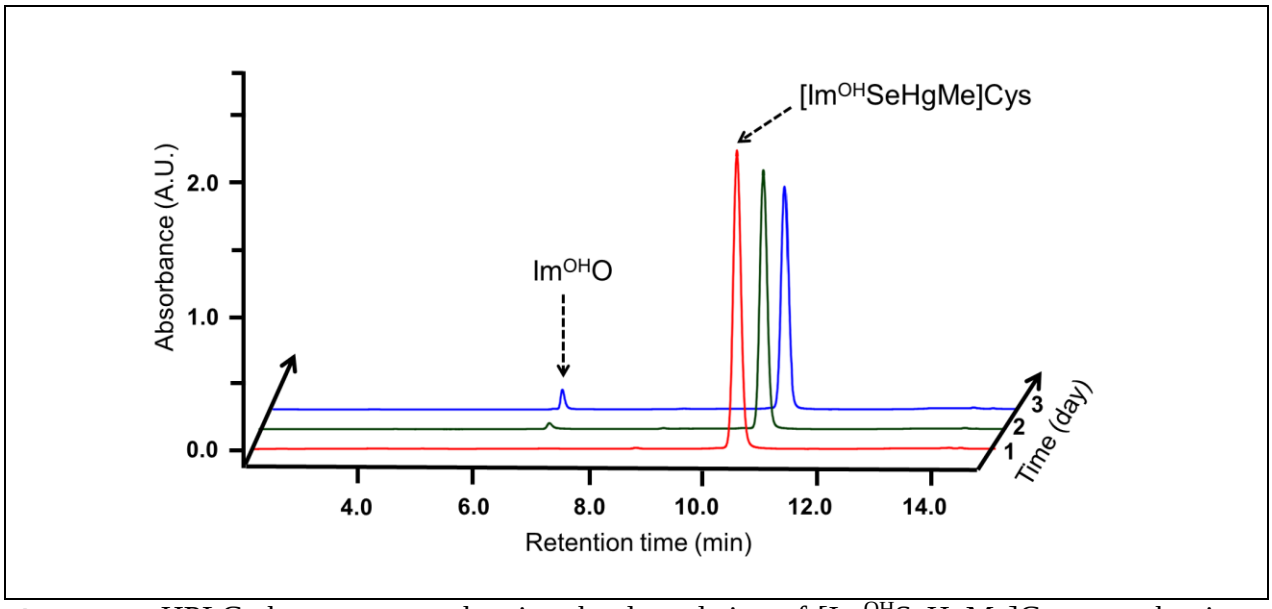

Figure S29. HPLC chromatogram showing the degradation of [Im^{OH}SeHgMe]Cys over the time (λ = 254 nm) at 37 °C in water-acetonitrile (1:1) mixture of pH 8.5.

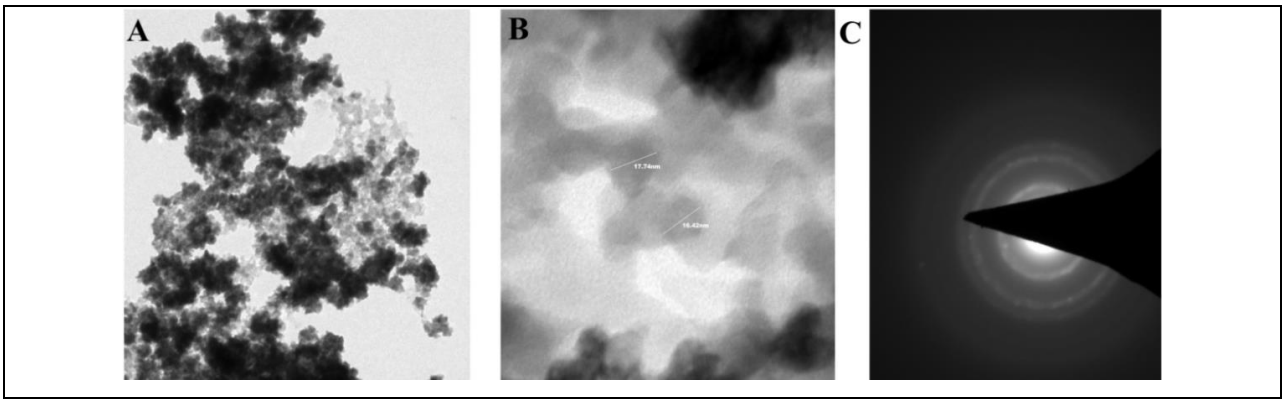

Figure S30. TEM (A), EDS and SAED (B) images of Hg(SeS) nanoparticles obtained in the reaction of MeHgCys/ $Im^{OH}Se$.

Synthesis of water-soluble (HgSeS) nanoparticles in the reaction of MeHgSG/ $Im^{OH}Se$:

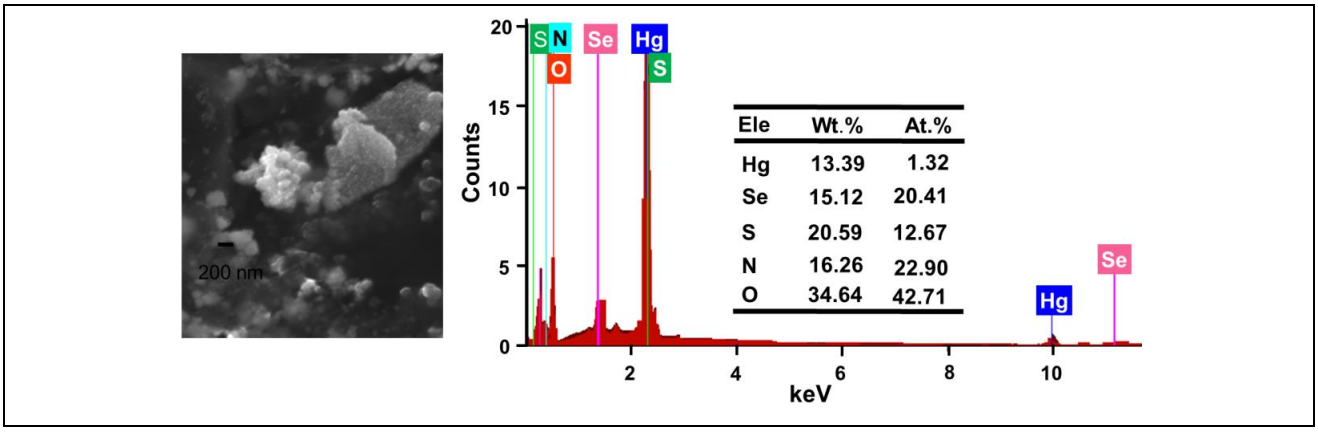

Figure S31. SEM image (A), EDS spectrum (B) of (HgSeS) nanoparticles obtained in the reaction of MeHgSG/ $Im^{OH}Se$.

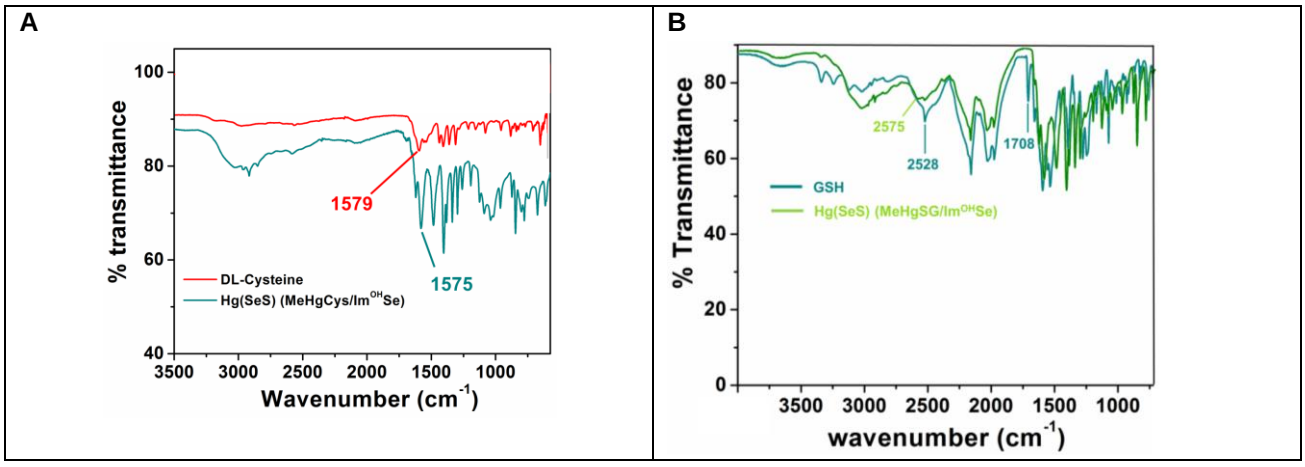

Figure S32. IR spectra of cysteine and cysteine capped Hg(SeS) NPs(A) and glutathione and glutathione capped Hg(SeS) NPs (B) obtained in the reactions of MeHgCys/$Im^{OH}Se$ and MeHgSG/$Im^{OH}Se$ respectively.

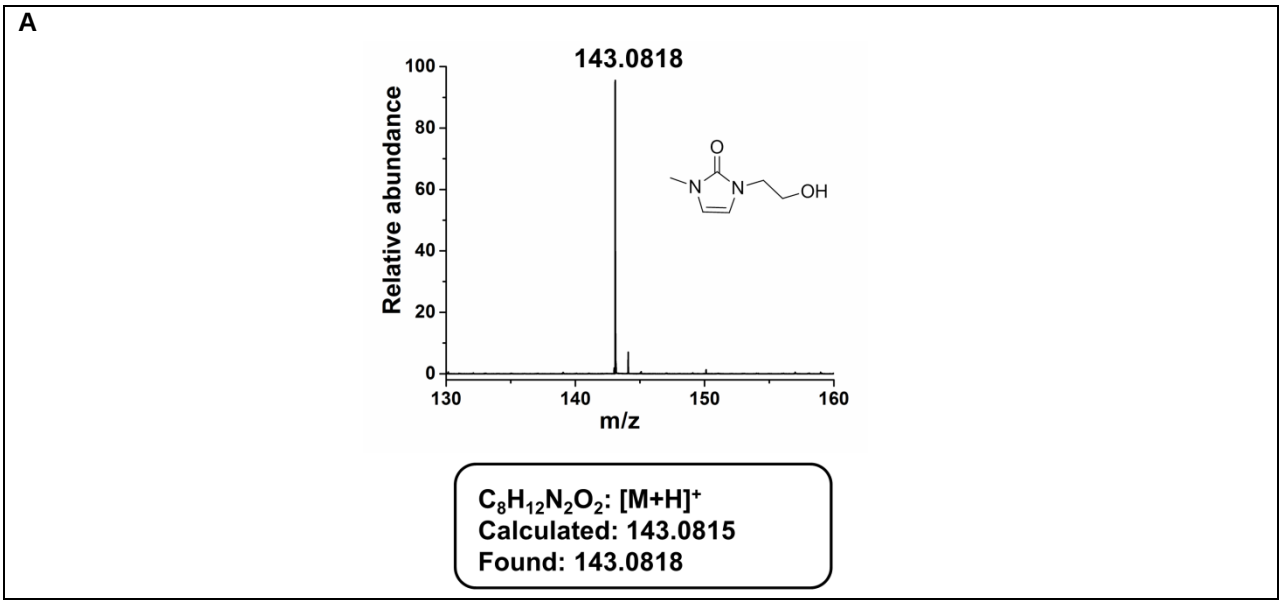

Figure S33. HRMS spectra of $Im^{OH}O$ obtained in the reaction of MeHgCys or MeHgSG with $Im^{OH}Se$

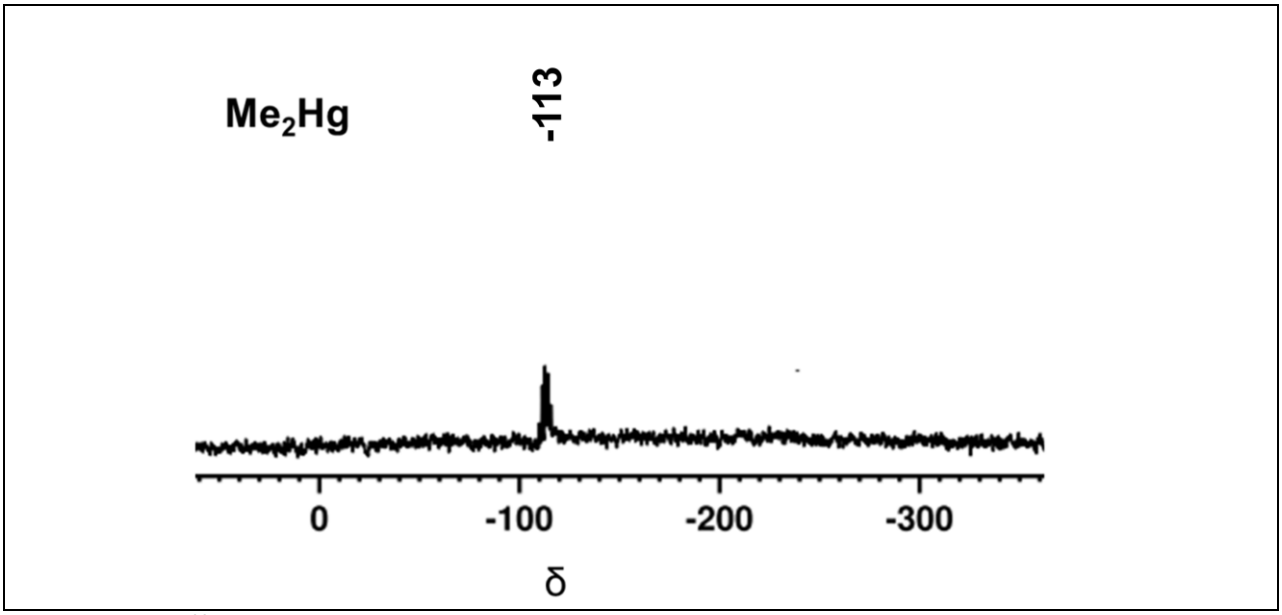

Figure S34. ^{199}Hg NMR spectra of Me_2Hg in DMSo-d_6 obtained in the reaction of MeHgCys or MeHgSG with $Im^{OH}Se$.

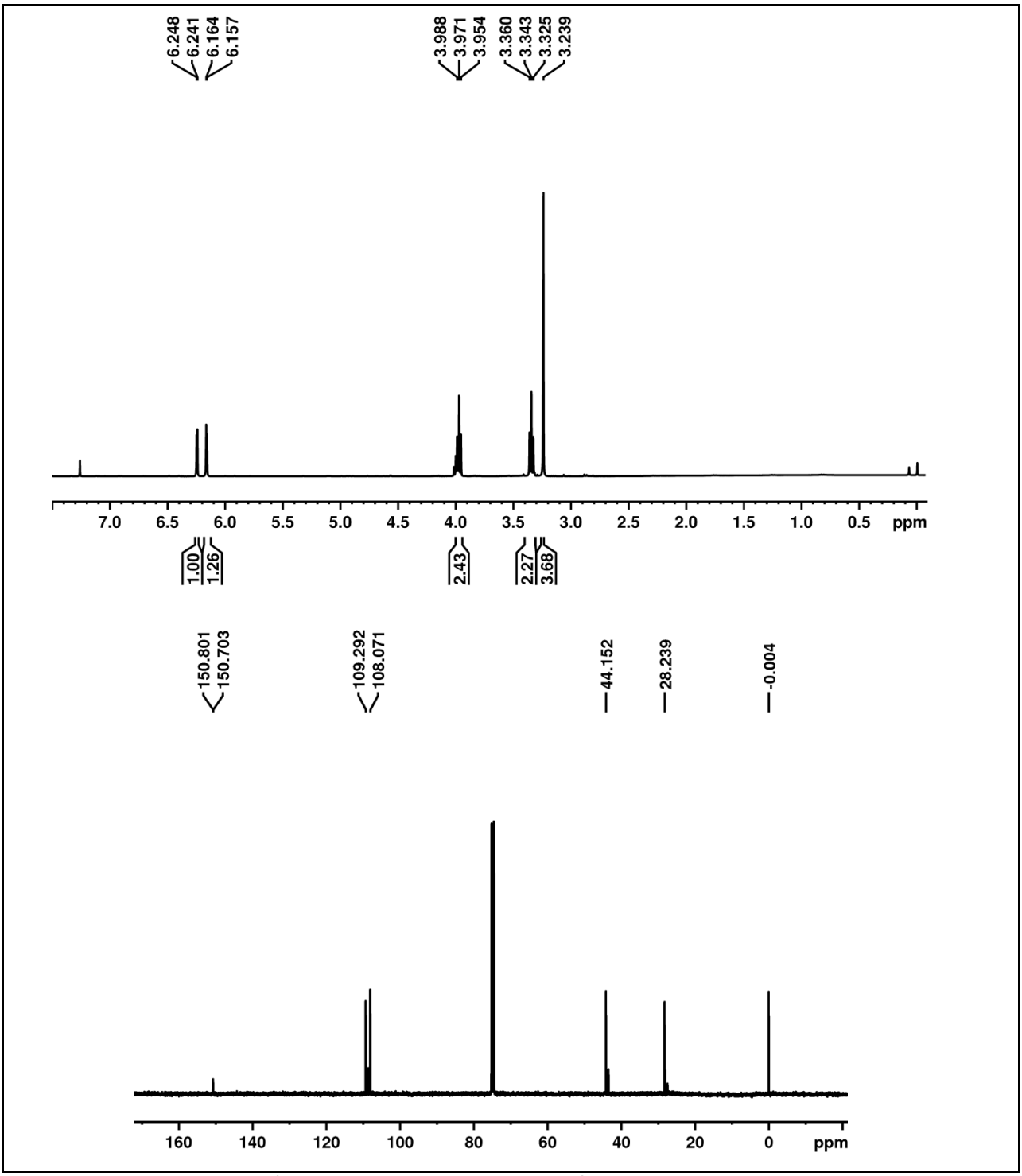

Figure S35. ^{1}H (top) and ^{13}C (bottom) NMR spectra of $Im^{OH}O$ in $CDCl_3$ obtained in the reaction of MeHgCys or MeHgSG with $Im^{OH}Se$.

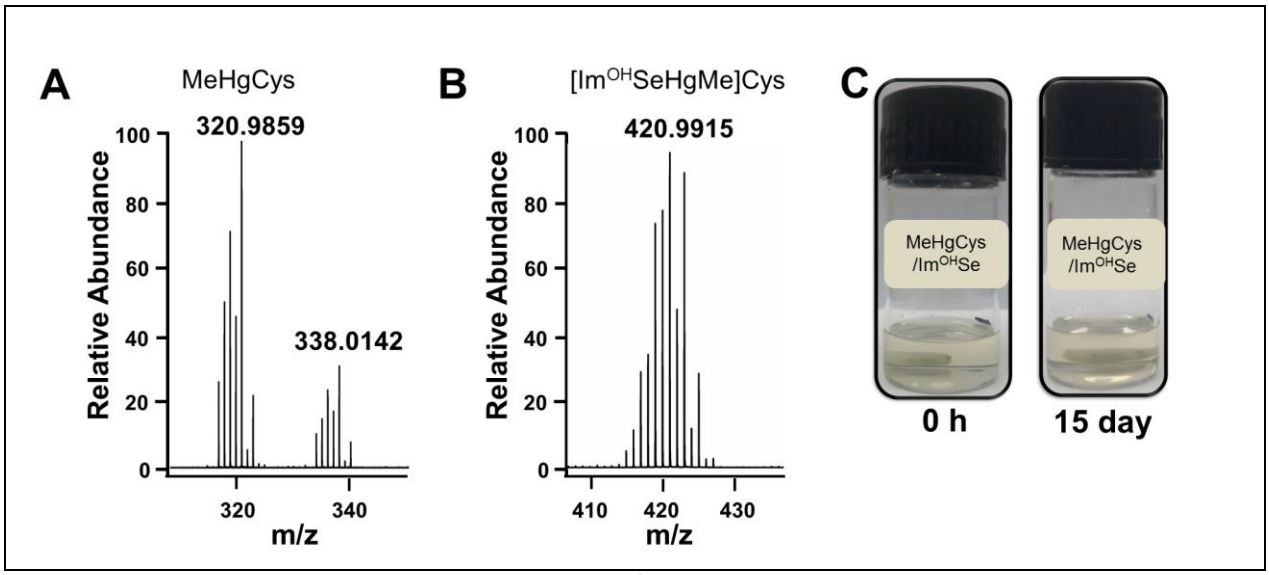

Figure S36. HRMS value for MeHgCys (A) and [Im^{OH}SeHgMe]Cys (B) and the reaction vial showing the formation of [Im^{OH}SeHgMe]Cys in the reaction between MeHgCys and Im^{OH}Se (C).

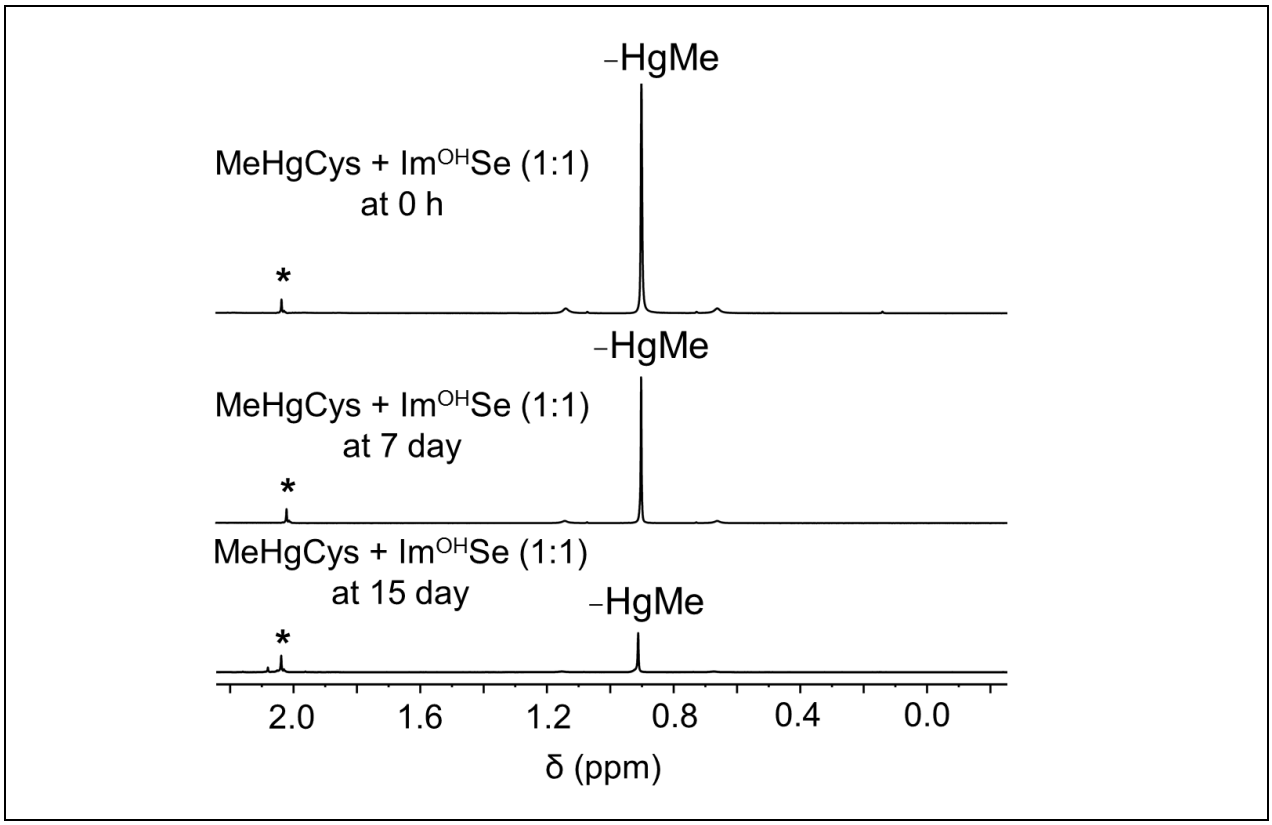

Figure S37. ^{1}H NMR spectra showing the cleavage of Hg–C bond of MeHgCys in the reaction of MeHgCys with Im^{OH}Se (1:1 molar ratio) in D_2O (pH = 7) at room temperature (23 °C). Mesitylene was used as external standard. (∗ = mesitylene peak).

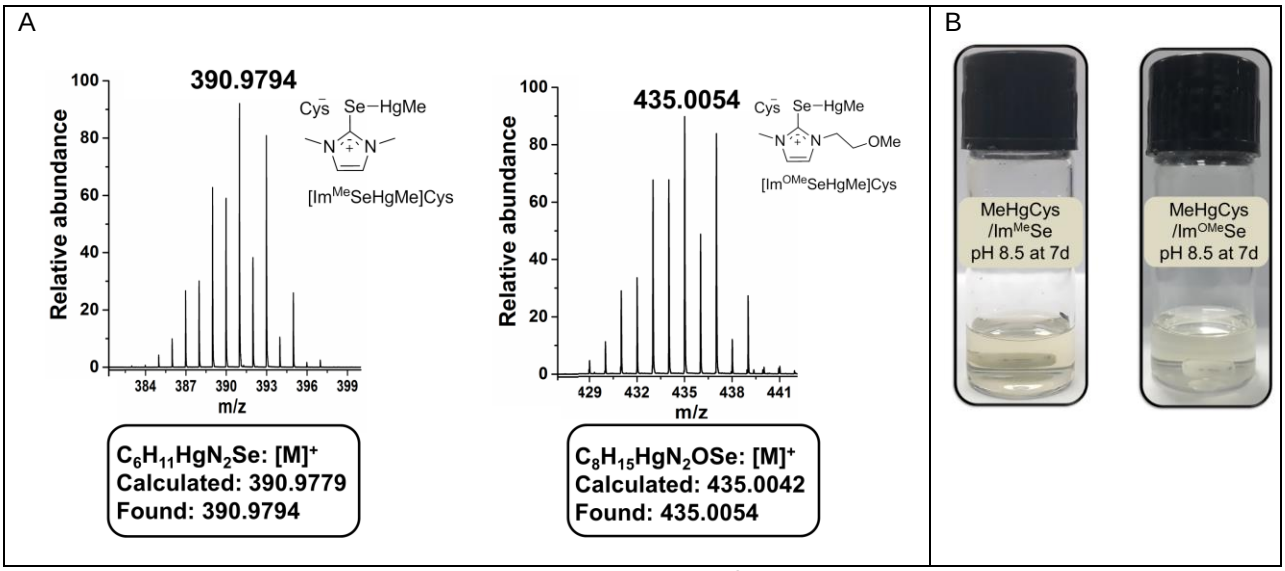

Figure S38. HRMS value for [Im^{Me}SeHgMe]Cys and [Im^{OMe}SeHgMe]Cys (A) obtained in the reaction between MeHgCys and Im^{Me}Se and Im^{OMe}Se respectively, (B) reaction vial showing that complexes [Im^{Me}SeHgMe]Cys (left) and [Im^{OMe}SeHgMe]Cys (right) are extremely stable even up to 7 days at 37 °C in pH 8.5.

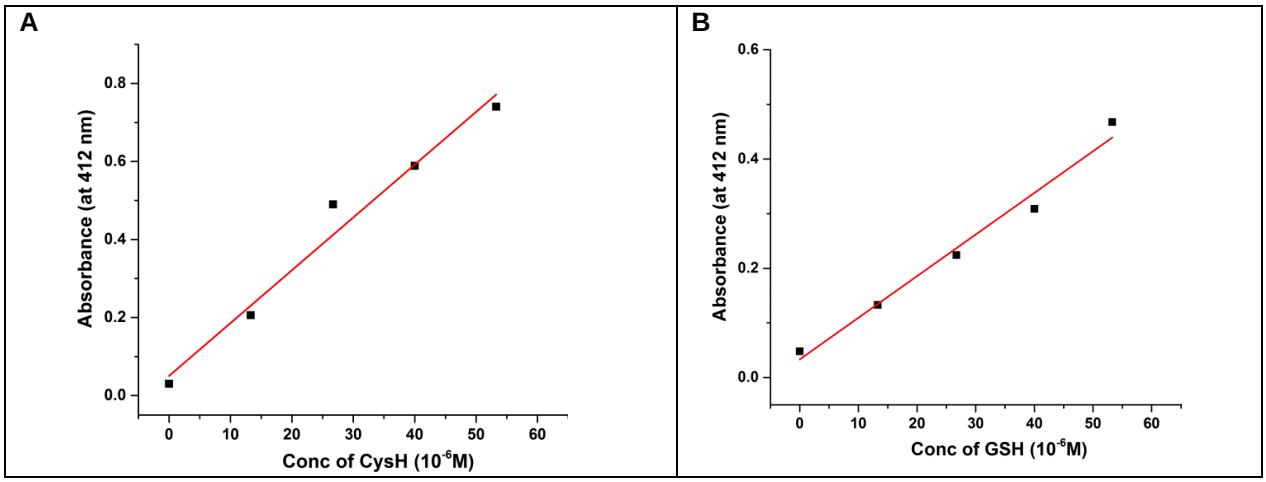

Figure S39. Standard calibration curve for cysteine (A) and glutathione (B) respectively to estimate the amount of free thiols present in the reaction solution of MeHgCys or MeHgSG treated with Im^{OH}Se.

Determination of the rate of degradation of MeHgCys (R = Me, Ar) by Im^{OH}Se:

General Procedure: A mixture of MeHgCys (30 mM) and calculated amount of imidazole-based selone (Im^{OH}Se**)** in 3 mL of water/acetonitrile mixture (1:1) or in PBS buffer (pH 8.5) stirred at 37°C. In case of water/acetonitrile mixture 2 equivalent of weak base $NaHCO_3$ or K_2HPO_4 was added after 1 h of stirring. An aliquot of 5 µl was taken from the above reaction mixture at various times and then diluted to 1 mL volume for HPLC analysis. Mobile phase: water/acetonitrile gradient.

VII. Computational Details:

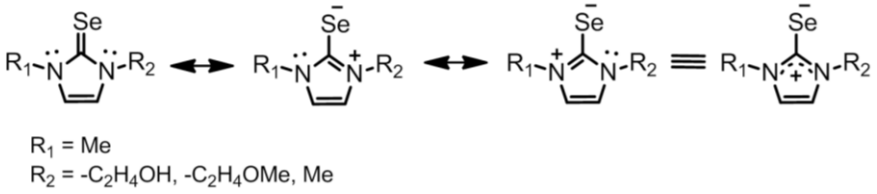

Figure S40. The principal resonance structures for imidazole-based selones Im^{Y}Se (where Y = OH, OMe and Me)

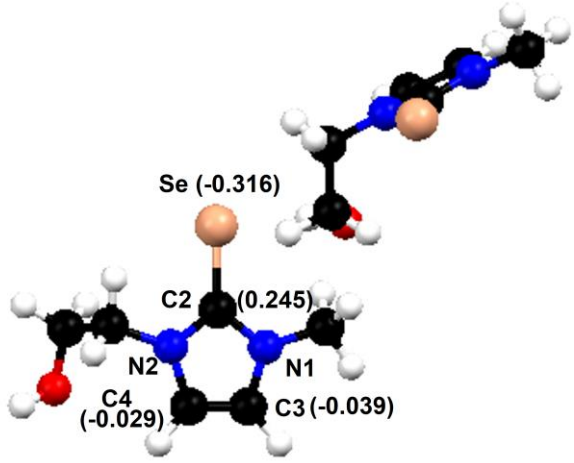

Im^{OH}Se

Charge on atoms (au) :
C2 = 0.245
Se = -0.316
N1 = -0.425; N2 = -0.435
C3 = -0.039; C4 = -0.029

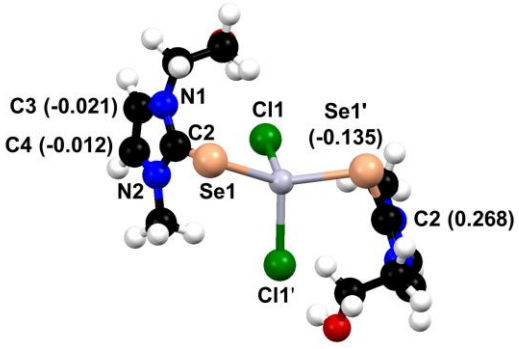

(Im^{OH}Se)$_2$HgCl$_2$

Charge on atoms (au) :
C2 = 0.268
Se = -0.135
N1 = -0.406; N2 = -0.395
C3 = -0.021; C4 = -0.012

Figure S41. The Natural Bond Orbitals (NBO) charges showing the increase of overall positive charge in the imidazole rings of (Im^{OH}Se)$_2$HgCl$_2$ compared to the free ligand Im^{OH}Se.

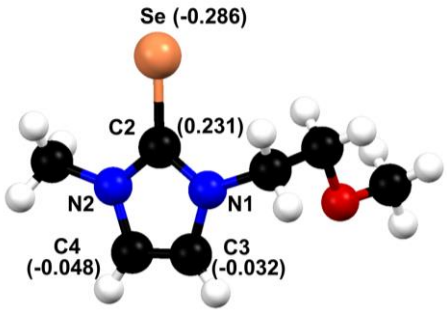 **$Im^{OMe}Se$**	**Charge on atoms (au) :** **C2 = 0.231** **Se = -0.286** **N1 = -0.440; N2 = -0.437** **C3 = -0.032; C4 = -0.048**
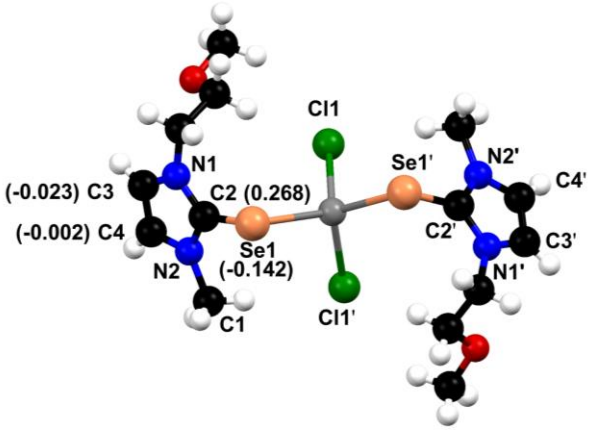 **$(Im^{OMe}Se)_2HgCl_2$**	**Charge on atoms (au) :** **C2 = 0.268** **Se = -0.142** **N1 = -0.406; N2 = -0.401** **C3 = -0.023; C4 = -0.002**

Figure S42. The Natural Bond Orbitals (NBO) charges showing the increase of overall positive charge in the imidazole rings of $(Im^{OMe}Se)_2HgCl_2$ compared to the free ligand $Im^{OMe}Se$.

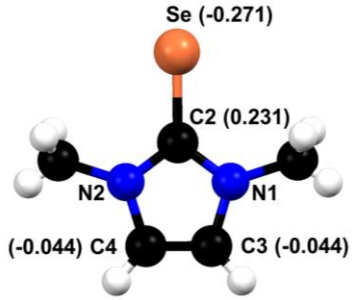 **Im^{Me}Se**	**Charge on atoms (au) :** **C2 = 0.231** **Se = -0.271** **N1 = -0.435; N2 = -0.435** **C3 = -0.044; C4 = -0.044**
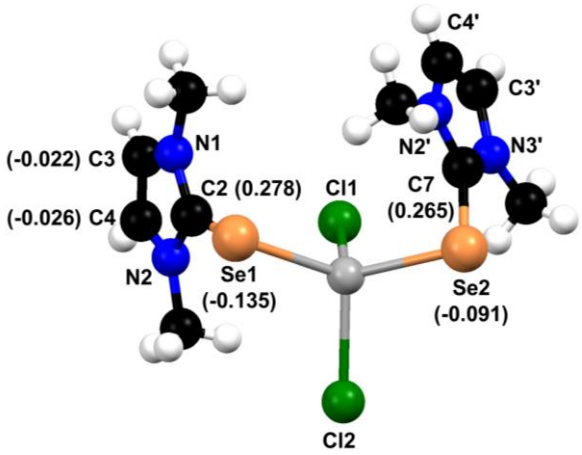 **(Im^{Me}Se)$_2$HgCl$_2$**	**Charge on atoms (au) :** **C2 = 0.278** **Se = -0.135** **N1 = -0.397; N2 = -0.399** **C3 = -0.022; C4 = -0.026**

Figure S43. The Natural Bond Orbitals (NBO) charges showing the increase of overall positive charge in the imidazole rings of (Im^{Me}Se)$_2$HgCl$_2$ compared to the free ligands Im^{Me}Se.

Crystal Packing of Im^{OH}Se and Im^{OMe}Se:

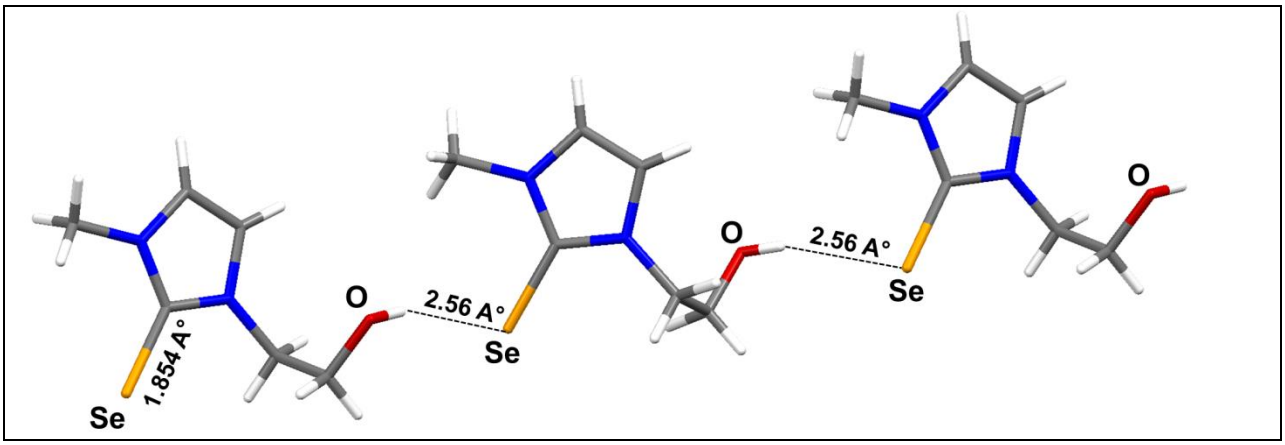

Figure S44. Crystal packing of Im^{OH}Se showing a chain-like structure due to the formation of OH⋯Se intermolecular hydrogen bonding interactions.

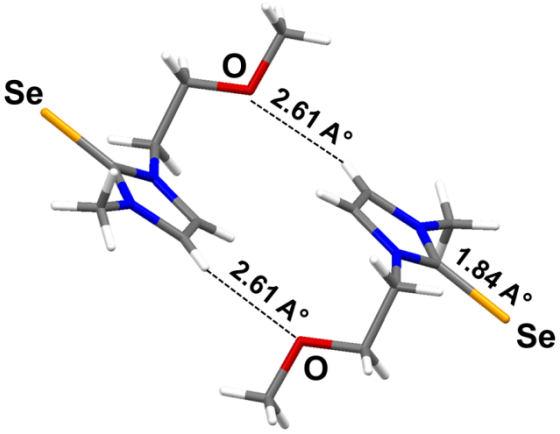

Figure S45. Crystal packing of $Im^{OMe}Se$ showing a dimeric structure due to formation of CH⋯O intermolecular hydrogen bonding interactions.

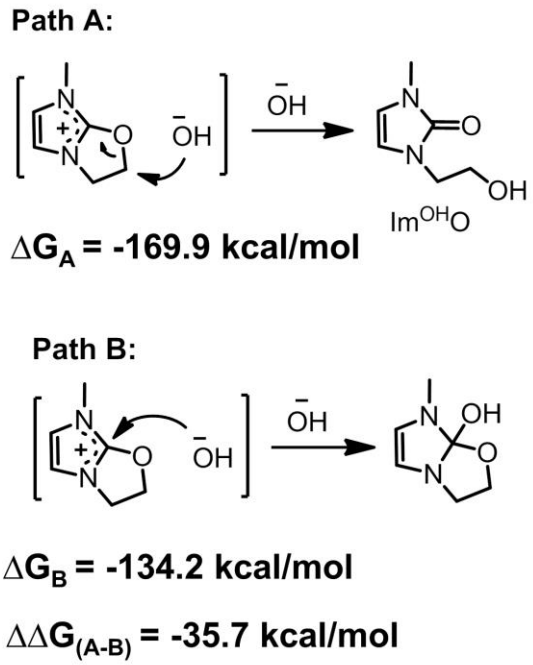

$\Delta\Delta G_{(A-B)}$ = -35.7 kcal/mol

Figure S46. Possible pathways of formation of $Im^{OH}O$ from intermediate **I** in the presence of hydroxide.

Table S5. The C–Se Bond Lengths, Bond Orders and Charge on Se Atom of $Im^{Y}Se$ (Y = OH, OMe and Me)

Compd	C–Se bond length (Å) (expt.)	C–Se bond length (Å) (calcd)	C–Se bond order (calcd)[a]	Charge on Se (au)[a]
$Im^{OH}Se$	1.854	1.856	1.274	-0.316
$Im^{OMe}Se$	1.837	1.843	1.340	-0.286
$Im^{Me}Se$	1.843	1.837	1.356	-0.271

[a]Optimization and natural bond orbitals (NBO) analysis was performed at the B3LYP/6-311++G(2d,p) level of theory (details are mentioned in the Experimental Section).

Optimized Geometries:

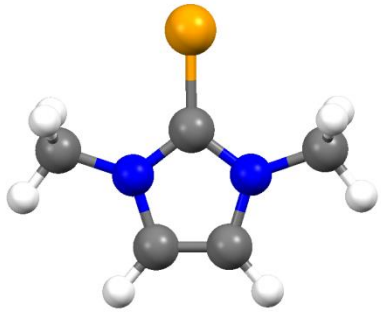

$Im^{Me}Se$

34	0.000041000	1.683808000	0.000000000
6	0.000000000	-0.153861000	0.000000000
7	1.085777000	-0.984184000	0.000000000
6	0.675624000	-2.305866000	0.000000000
6	2.461410000	-0.518991000	0.000000000
1	1.373933000	-3.123423000	0.000000000
1	3.120256000	-1.385997000	0.000000000
1	2.649609000	0.091890000	0.882891000
7	-1.085827000	-0.984132000	0.000000000
6	-0.675741000	-2.305829000	0.000000000
1	2.649609000	0.091890000	-0.882891000
6	-2.461434000	-0.518865000	0.000000000
1	-1.374085000	-3.123357000	0.000000000
1	-3.120327000	-1.385836000	0.000000000
1	-2.649601000	0.092026000	0.882891000
1	-2.649601000	0.092026000	-0.882891000

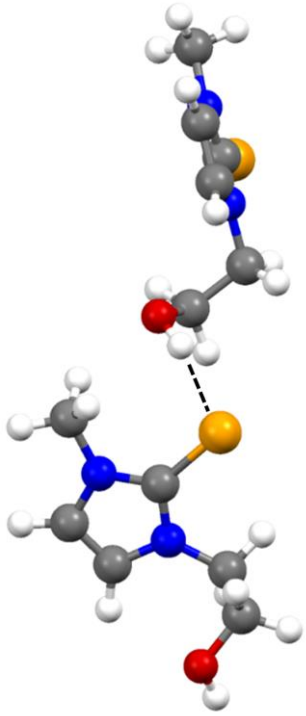

$Im^{OH}Se$

34	2.457019000	0.837129000	-1.192458000
7	3.307180000	0.864002000	1.570378000
7	4.333708000	-0.663218000	0.418519000
8	7.175549000	-1.069419000	-0.489198000
1	7.559710000	-1.950604000	-0.543230000
6	3.396711000	0.326318000	0.324876000
6	4.176845000	0.214465000	2.429443000
1	4.263319000	0.485575000	3.466428000
6	4.819696000	-0.731979000	1.712210000
1	5.588375000	-1.426619000	1.996490000
6	2.414919000	1.953751000	1.946626000
1	2.493225000	2.752432000	1.210501000
1	2.720387000	2.321575000	2.924559000
1	1.381924000	1.606351000	1.982880000
6	4.764246000	-1.503207000	-0.691760000
1	3.951641000	-1.507052000	-1.420023000
1	4.901835000	-2.518898000	-0.313023000
6	6.042344000	-0.998711000	-1.353385000
1	6.211036000	-1.565513000	-2.275110000
1	5.921603000	0.050658000	-1.623676000
34	-4.998541000	-1.729937000	0.285182000
7	-5.119307000	1.110959000	-0.133943000
7	-3.146740000	0.322892000	-0.584715000
8	-0.428175000	0.646857000	0.645510000
1	0.317889000	0.715987000	0.017138000
6	-4.394392000	-0.044600000	-0.159687000
6	-4.331102000	2.178265000	-0.534691000
1	-4.709250000	3.183893000	-0.581023000
6	-3.103823000	1.687283000	-0.810558000
1	-2.202665000	2.183405000	-1.120909000
6	-6.518218000	1.186899000	0.246618000

	1	-6.653724000	0.786169000	1.251101000
	1	-6.827436000	2.230547000	0.217065000
	1	-7.129073000	0.599232000	-0.439212000
	6	-2.025551000	-0.592778000	-0.750933000
	1	-2.449635000	-1.588360000	-0.891328000
	1	-1.486030000	-0.306561000	-1.656491000
	6	-1.081557000	-0.599112000	0.448080000
	1	-0.354073000	-1.407378000	0.307630000
	1	-1.650861000	-0.810879000	1.354403000

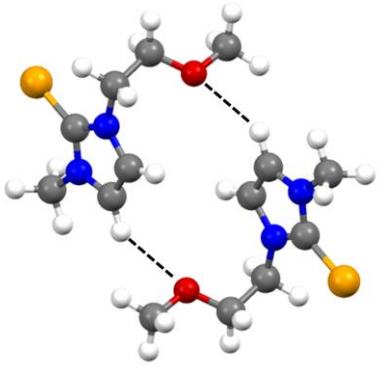 $Im^{OMe}Se$	34	-5.593482000	0.064320000	0.020660000
	8	-1.561813000	-2.716832000	0.225187000
	7	-2.815848000	-0.210613000	-0.737324000
	7	-3.219528000	1.673003000	0.264332000
	6	-3.816700000	0.520132000	-0.156575000
	6	-2.986742000	-1.539396000	-1.307861000
	1	-2.225931000	-1.670962000	-2.078806000
	1	-3.974030000	-1.573853000	-1.770568000
	6	-1.620960000	0.483986000	-0.673999000
	1	-0.703670000	0.083740000	-1.065429000
	6	-2.889199000	-2.650079000	-0.277761000
	1	-3.600469000	-2.461579000	0.534250000
	1	-3.162206000	-3.600892000	-0.756889000
	6	-1.869940000	1.656428000	-0.051643000
	1	-1.202456000	2.462006000	0.198935000
	6	-3.921963000	2.755304000	0.931424000
	1	-4.689646000	3.166643000	0.275648000
	1	-3.199866000	3.528422000	1.188524000
	1	-4.408280000	2.383724000	1.833274000
	6	-1.441136000	-3.631345000	1.302090000
	1	-2.098315000	-3.352055000	2.134002000

	1	-0.406173000	-3.600931000	1.641151000
	1	-1.686661000	-4.653251000	0.986689000
	34	5.593062000	-0.068169000	-0.025590000
	8	1.565245000	2.719895000	-0.219048000
	7	2.817720000	0.211559000	0.738938000
	7	3.215415000	-1.672065000	-0.265096000
	6	3.815806000	-0.520682000	0.155319000
	6	2.992390000	1.539707000	1.309785000
	1	2.233956000	1.672070000	2.082931000
	1	3.981043000	1.572262000	1.769703000
	6	1.621355000	-0.480694000	0.677865000
	1	0.705758000	-0.078949000	1.071717000
	6	2.893761000	2.651146000	0.280598000
	1	3.602791000	2.462261000	-0.533282000
	1	3.169168000	3.601302000	0.759661000
	6	1.866595000	-1.653140000	0.054026000
	1	1.196866000	-2.457177000	-0.195551000
	6	3.914240000	-2.755275000	-0.934497000
	1	4.681562000	-3.169650000	-0.280199000
	1	3.189801000	-3.526090000	-1.191926000
	1	4.400537000	-2.383623000	-1.836318000
	6	1.443023000	3.635560000	-1.294773000
	1	2.098077000	3.356471000	-2.128435000
	1	0.407283000	3.606454000	-1.631570000
	1	1.690207000	4.656934000	-0.978936000

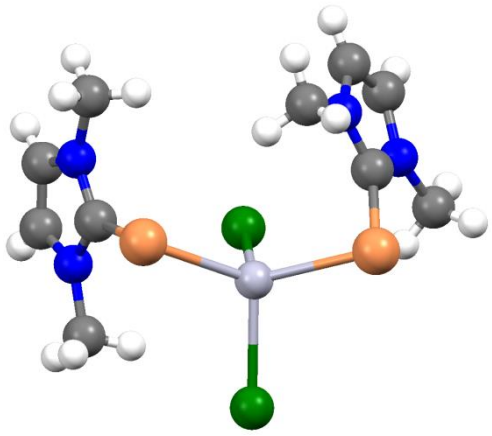

$(Im^{Me}Se)_2HgCl_2$

80	-0.111031000	-0.915381000	-0.101965000
34	-2.622695000	-0.816769000	-0.727859000
34	1.866928000	-0.078398000	-1.564964000
17	0.330571000	-3.322034000	0.642850000
17	0.078786000	0.515189000	2.016322000
7	-3.213255000	1.292624000	1.129194000
7	-2.348639000	2.046608000	-0.688395000
6	-2.736202000	0.924665000	-0.063799000
7	3.039429000	2.043776000	-0.003375000
7	3.448936000	0.106561000	0.853149000
6	-3.094746000	2.659569000	1.256515000
1	-3.341702000	3.164999000	1.997159000
6	-2.564136000	3.127137000	0.129064000
1	-2.373517000	4.015153000	-0.065815000
6	2.828773000	0.726591000	-0.164610000
6	-1.753827000	2.081673000	-2.021580000
1	-0.886887000	1.668148000	-1.996771000
1	-1.663907000	2.993770000	-2.308687000
1	-2.316979000	1.605253000	-2.636510000
6	-3.700489000	0.373543000	2.141407000
1	-4.447908000	-0.118893000	1.792338000
1	-3.976842000	0.867781000	2.915985000
1	-3.000878000	-0.237662000	2.383031000
6	3.777360000	2.256250000	1.133848000
1	4.049052000	3.080606000	1.469690000
6	2.566531000	3.095997000	-0.895288000
1	3.019996000	3.027871000	-1.738799000
1	2.746193000	3.954406000	-0.503581000
1	1.621492000	2.998776000	-1.031975000
6	4.031413000	1.062523000	1.666297000
1	4.513907000	0.900299000	2.444742000

	6	3.451628000	-1.318636000	1.099723000
	1	2.582194000	-1.592738000	1.401346000
	1	4.102894000	-1.525377000	1.773058000
	1	3.669296000	-1.782691000	0.288565000
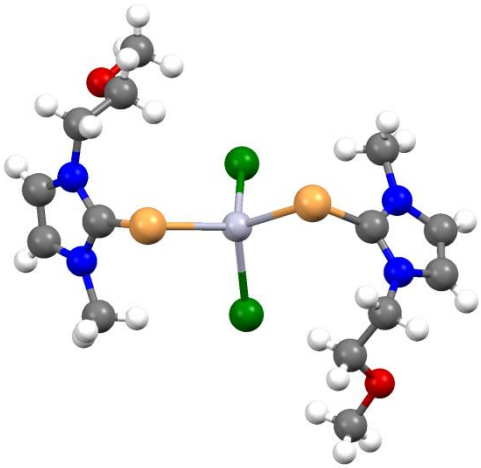 $(Im^{OMe}Se)_2HgCl_2$	80	0.000020000	-0.000463000	0.026222000
	34	-1.804230000	-1.078443000	1.569248000
	17	-0.850336000	1.751004000	-1.581820000
	7	-3.359394000	-2.271938000	-0.523722000
	8	-4.837966000	2.159948000	-0.784827000
	7	-4.309454000	-0.493360000	0.278236000
	6	-3.215115000	-1.284487000	0.362254000
	6	-4.570239000	-2.089591000	-1.178726000
	1	-4.918517000	-2.633791000	-1.848713000
	6	-4.063470000	1.953761000	0.373177000
	1	-4.144007000	2.714456000	0.968159000
	1	-3.129003000	1.850816000	0.133179000
	6	-4.556658000	0.714507000	1.055207000
	1	-4.120855000	0.632165000	1.917209000
	1	-5.510085000	0.799546000	1.212205000
	6	-5.145308000	-0.997343000	-0.679752000
	1	-5.967377000	-0.641221000	-0.934760000
	6	-2.428008000	-3.368960000	-0.752697000
	1	-1.547406000	-3.015052000	-0.905705000
	1	-2.708166000	-3.872360000	-1.521684000
	1	-2.411679000	-3.942991000	0.016317000
	6	-4.473297000	3.348411000	-1.462856000
	1	-4.716620000	4.108342000	-0.930874000
	1	-4.929728000	3.388700000	-2.307857000
	1	-3.524898000	3.353037000	-1.611857000
	34	1.804204000	1.079004000	1.569195000
	17	0.850307000	-1.750593000	-1.581737000

	7	3.360106000	2.271727000	-0.523835000
	8	4.838678000	-2.160172000	-0.784729000
	7	4.308755000	0.493120000	0.278207000
	6	3.215087000	1.284991000	0.362189000
	6	4.570210000	2.090021000	-1.178831000
	1	4.917815000	2.633448000	-1.848844000
	6	4.063443000	-1.953257000	0.373266000
	1	4.143980000	-2.713923000	0.968284000
	1	3.128303000	-1.851064000	0.133264000
	6	4.556632000	-0.713970000	1.055236000
	1	4.121570000	-0.632260000	1.917234000
	1	5.510059000	-0.799002000	1.212238000
	6	5.145279000	0.997796000	-0.679805000
	1	5.967348000	0.641662000	-0.934797000
	6	2.427979000	3.369410000	-0.752860000
	1	1.547378000	3.015495000	-0.905851000
	1	2.708137000	3.872773000	-1.521873000
	1	2.412392000	3.942806000	0.016126000
	6	4.472596000	-3.348735000	-1.462701000
	1	4.716660000	-4.109313000	-0.930683000
	1	4.929026000	-3.389064000	-2.307700000
	1	3.524869000	-3.352628000	-1.611700000
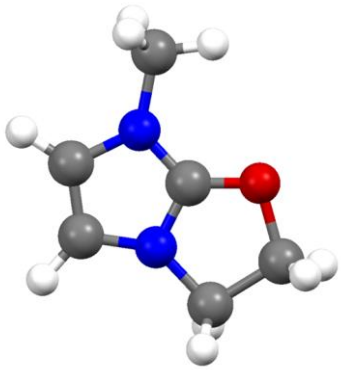 G = -418.538595 HF	6	-0.018856000	-0.344241000	-0.004754000
	7	0.603984000	0.828351000	-0.024619000
	7	-1.335348000	-0.175099000	-0.000394000
	6	-0.353577000	1.837914000	-0.016031000
	6	-1.555018000	1.213238000	-0.007782000
	6	-2.356488000	-1.229204000	0.010485000
	1	-1.858518000	-2.195708000	0.010548000
	1	-2.966688000	-1.134291000	0.907003000
	1	-2.979389000	-1.140678000	-0.877888000

	6	2.055975000	0.635757000	0.064891000
	1	2.572666000	1.141197000	-0.748848000
	1	2.430317000	1.001378000	1.020663000
	6	2.137394000	-0.915496000	-0.061134000
	8	0.739425000	-1.413521000	0.034575000
	1	2.691915000	-1.386988000	0.744166000
	1	2.515453000	-1.240809000	-1.027049000
	1	-2.551589000	1.618910000	-0.015080000
	1	-0.106603000	2.884582000	-0.029077000
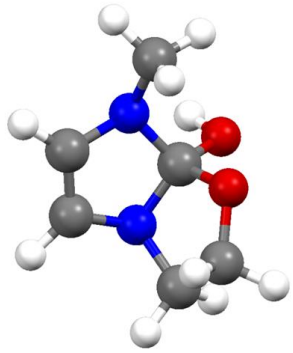 **G = -494.588140 HF**	6	-0.095878000	-0.437014000	0.386973000
	7	0.796859000	0.691417000	0.669978000
	7	-1.381240000	0.185655000	0.121117000
	6	0.139875000	1.841296000	0.152519000
	6	-1.124226000	1.539379000	-0.156726000
	6	-2.345792000	-0.560726000	-0.674298000
	1	-2.465275000	-1.556522000	-0.248390000
	1	-3.309230000	-0.050892000	-0.629800000
	1	-2.039618000	-0.661276000	-1.721317000
	6	2.097139000	0.308996000	0.108308000
	1	2.677515000	1.190252000	-0.160891000
	1	2.652483000	-0.268279000	0.849166000
	6	1.711053000	-0.561676000	-1.091842000
	8	0.452143000	-1.139903000	-0.721935000
	1	2.419269000	-1.369391000	-1.278932000
	1	1.584036000	0.029262000	-2.003731000
	8	-0.175553000	-1.393607000	1.401134000
	1	-0.628528000	-0.972660000	2.142866000
	1	-1.922753000	2.199486000	-0.456228000
	1	0.617021000	2.807063000	0.186390000

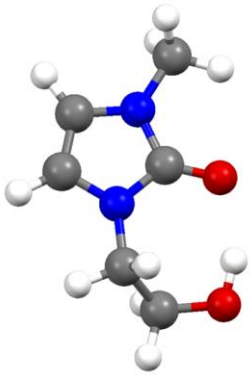 G = -494. 645031 HF	8	0.065576000	-1.569643000	-0.287964000
	7	-1.774656000	-0.165052000	0.047444000
	7	0.199915000	0.773679000	-0.149892000
	8	2.766174000	-1.145645000	0.100863000
	1	1.882357000	-1.544119000	-0.023626000
	6	-0.438995000	-0.452105000	-0.148892000
	6	-1.951105000	1.210207000	0.157126000
	6	-0.739311000	1.785403000	0.031484000
	6	1.621780000	0.973281000	-0.435380000
	1	1.805478000	2.043389000	-0.323480000
	1	1.827870000	0.701252000	-1.474578000
	6	-2.800416000	-1.184548000	0.128397000
	1	-3.542469000	-1.051039000	-0.661534000
	1	-3.299148000	-1.156613000	1.099438000
	1	-2.314708000	-2.150205000	0.003040000
	6	2.575376000	0.197901000	0.479222000
	1	3.556137000	0.677339000	0.422228000
	1	2.224705000	0.284594000	1.518001000
	1	-2.917178000	1.653266000	0.323185000
	1	-0.457818000	2.823224000	0.059525000
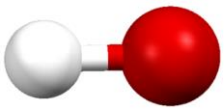 G = -75.835618 HF	8	0.000000000	0.000000000	0.107472000
	1	0.000000000	0.000000000	-0.859777000

Full citations of reference 57**:**

Gaussian 09, Revision A.02, M. J. Frisch, G. W. Trucks, H. B. Schlegel, G. E. Scuseria, M. A. Robb, J. R. Cheeseman, G. Scalmani, V. Barone, B. Mennucci, G. A. Petersson, H. Nakatsuji, M. Caricato, X. Li, H. P. Hratchian, A. F. Izmaylov, J. Bloino, G. Zheng, J. L. Sonnenberg, M. Hada, M. Ehara, K. Toyota, R. Fukuda, J. Hasegawa, M. Ishida, T. Nakajima, Y. Honda, O. Kitao, H. Nakai, T. Vreven, J. A. Montgomery, Jr., J. E. Peralta, F. Ogliaro, M. Bearpark, J. J.

Heyd, E. Brothers, K. N. Kudin, V. N. Staroverov, R. Kobayashi, J. Normand, K. Raghavachari, A. Rendell, J. C. Burant, S. S. Iyengar, J. Tomasi, M. Cossi, N. Rega, J. M. Millam, M. Klene, J. E. Knox, J. B. Cross, V. Bakken, C. Adamo, J. Jaramillo, R. Gomperts, R. E. Stratmann, O. Yazyev, A. J. Austin, R. Cammi, C. Pomelli, J. W. Ochterski, R. L. Martin, K. Morokuma, V. G. Zakrzewski, G. A. Voth, P. Salvador, J. J. Dannenberg, S. Dapprich, A. D. Daniels, O. Farkas, J. B. Foresman, J. V. Ortiz, J. Cioslowski, and D. J. Fox, Gaussian, Inc., Wallingford CT, 2009.